EXTREME ENSO (El Nino Southern Oscillation) EVENTS

AND

MONSOON VARIABILITY OVER INDIA

by

ATHIRA K.S

(2015-20-023)

THESIS

submitted in partial fulfilment of the

requirement of the degree of

B. Sc.-M. Sc. (Integrated) Climate Change Adaptation

Faculty of Agriculture

Kerala Agricultural University

ACADEMY OF CLIMATE CHANGE EDUCATION AND RESEARCH

VELLANIKKARA, THRISSUR - 680 656

KERALA, INDIA,

2020

DECLARATION

I, hereby declare that this thesis entitled **"EXTREME ENSO (El Niño Southern Oscillation) EVENTS AND MONSOON VARIABILITY OVER INDIA"** is a bonafide record of research work done by me during the course of research and the thesis has not previously formed the basis for the award to me of any degree, diploma, associateship, fellowship or other similar title, of any other University or Society.

Vellanikkara, **Athira K.S**

Date: (2015-20-023)

CERTIFICATE

Certified that this thesis entitled **"EXTREME ENSO (El Nino Southern Oscillation) EVENTS AND MONSOON VARIABILITY OVER INDIA"** is a record of research work done independently by Ms. Athira K.S (2015-20-023) under my guidance and supervision and that it has not previously formed the basis for the award of any degree, diploma, fellowship or associateship to her.

Vellanikkara,

Date:

Dr.P.O. Nameer

(Major Advisor)

Special Officer

Academy of Climate Change Education and Research

Kerala Agricultural University

Vellanikkara, Thrissur

CERTIFICATE

We, the undersigned members of the advisory committee of **Athira K.S (2015-20-023)**, a candidate for the degree of **B. Sc. -M. Sc. (Integrated) Climate Change Adaptation**, agree that the thesis entitled **"EXTREME ENSO (El Nino Southern Oscillation) EVENTS AND MONSOON VARIABILITY OVER INDIA"** may be submitted by Ms. Athira K.S., in partial fulfilment of the requirement for the degree.

Dr.P.O. Nameer
(Chairman, Advisory Committee)
Special Officer
ACCER, KAU
Vellanikkara, Thrissur

Dr. Roxy Mathew Koll
(Member, Advisory Committee)
Scientist E
Ocean Atmosphere Dynamics and Interaction
IITM, Pune

Dr. T.K. Kunhamu
(Member, Advisory Committee)
Professor and Head
Dept. of Silviculture and Agroforestry
College of Forestry
KAU, Vellanikkara

Dr. M. Shaji
(Member, Advisory Committee)
Dept. of Wildlife Science
College of Forestry
KAU, Vellanikkara

EXTERNAL EXAMINER

ACKNOWLEDGEMENT

I take this opportunity to acknowledge the valuable assistance extended to me from various quarters during the preparation of this thesis entitled **"EXTREME ENSO (El Nino Southern Oscillation) EVENTS AND MONSOON VARIABILITY OVER INDIA"**.

First of all, I express my sincere gratitude to my major adviser **Dr. P.O. Nameer** (Special Officer, ACCER, KAU) for his guidance and timely enquiry to track the progress of the thesis so that it was completed within the scheduled time.

I am really fortunate to have completed my thesis at IITM, Pune under the exemplary supervision of **Dr. Roxy Mathew Koll** (Scientist E). I sincerely acknowledge for accepting me as his student and for all the efforts to ensure the project position at IITM. I deeply thank him for the careful monitoring and the weekly conduction of group meetings which helped me to gather new ideas. I would also like to convey my regards for reviewing the thesis and the valuable comments given.

I am extremely thankful to **Shri. Panini Dasgupta** (Senior Research Fellow IITM) who wholeheartedly helped at every phase of my thesis preparation. I am grateful for his encouragement, suggestions and discussions which paved way to shape the thesis. I am indebted to him for the huge amount of precious time in teaching python language and the efforts put towards this endeavour.

I pay my warm gratitude for all the facilities offered by IITM (Indian Institute of Tropical Meteorology) and CCCR (Centre for Climate Change Research). I am grateful to the Director of IITM for providing the requisite infrastructure resources and the accommodation at Prithvi – The Hall of Residence.

I thank my classmates as well as the teaching and non-teaching staffs at ACCER for supporting me to successfully complete the graduation and post-graduation degree.

I sincerely convey my gratefulness to my friends at IITM for the memorable fun filled days in Pune.

Last but not the least I extend the heartfelt acknowledgement towards my parents and my sister for their motivation, support, love, care and prayers without whom I would never have enjoyed this opportunity.

ATHIRA K.S

TABLE OF CONTENTS

LIST OF FIGURES

LIST OF FIGURES

LIST OF FIGURES

LIST OF FIGURES

LIST OF FIGURES

SYMBOLS AND ABBREVIATIONS

AMO	Atlantic Meridional Oscillation
AZM	Atlantic Zonal Mode
CP	Central Pacific
CT	Cold Tongue
DJF	December, January, February
EIOD	Early Indian Ocean Dipole
ENSO	El Niño–Southern Oscillation
EP	Eastern Pacific
EQUINOO	Equatorial Indian Ocean Oscillation
GDP	Gross Domestic Product
IMD	India Meteorological Department
IOD	Indian Ocean Dipole
ISMR	Indian Summer Monsoon Rainfall
ITCZ	Inter Tropical Convergence Zone
JJAS	June, July, August, September
EOF	Empirical Orthogonal Function
LLJ	Low Level Jet streams
NCEP	National Center for Environmental Prediction
NCAR	National Center for Atmospheric Research

NOAA	National Oceanic and Atmospheric Administration
PC1	First Principal Component
PC2	Second Principal Component
PDO	Pacific Decadal Oscillation
PIOD	Prolonged Indian Ocean Dipole
SST	Sea Surface Temperature
WP	Warm Pool
WWE	Westerly Wind Events

CHAPTER 1

INTRODUCTION

Rainfall is undoubtedly an inevitable part of our lives. It affects every strata of livelihood as well as the overall growth of a nation. The southwest monsoon from June to September constitutes the primary source of rainfall for our country. Agriculture which is amongst the major contributors to Gross Domestic Product (GDP) is primarily dependent on the southwest monsoon. All the major agricultural activities are centered upon the onset of monsoon. With the high density of the population mainly employed in the agriculture sector, monsoon and its variability are critical for their daily bread.

The Indian monsoon is a highly variable phenomenon with variations in the amount of rainfall received in different parts of the subcontinent. There are years when the rainfall received is particularly high which may lead to flood conditions and reduced rainfall years which in turn leads to severe droughts. These fluctuations in precipitation can have a profound impact on the lives of people. The geographical features of our country are one of its kind and have a great hold on monsoon. The vast stretches of the Western Ghats, the snow-covered Himalayas, are beneficial in bringing orographic rainfall. Tibetan plateau acts as a heat source which creates a low-pressure system. These along with oceanic and atmospheric circulation patterns influence the monsoon behaviour.

There are different causes responsible for this asymmetric rainfall conditions ranging from local to global phenomenon. Under the climate change scenario there is more possibility that the variations in rainfall may increase further. Among the reasons for monsoon variability one of the most important and that which has a wide influence is the El Niño Southern Oscillation (ENSO). It is unique to the tropical Pacific Ocean and has a great impact on the Indian monsoon circulations. ENSO has two phases – a warm phase named El Niño and a cold phase which is characterised by basin-wide cooling of the tropical Pacific Ocean, called the La Niña (Philander 1998).

The oscillation refers to the seesaw pattern of the atmospheric pressure in western and eastern Pacific (Aceituno 1992), which takes place on an appropriate time scale of 2 to 7 years. Under normal conditions the trade winds blow from east Pacific to the west Pacific, carrying the warm Equatorial water. Upwelling occurs over the eastern Pacific, to substitute this loss of water. Cold and nutrient rich water reach the surface making the region highly productive for fisheries. The difference in the temperature between the east and west Pacific further enhances the trade winds due to the pressure difference created. Warm water is piled up over the west and warm air ascends here leading to formation of towering clouds and rainfall. The air descends over eastern Pacific, thus completing the circulation. This is termed as the Walker circulation.

Intense rainfall occurs over the western Pacific whereas drought prevails over the eastern Pacific. When the trade wind weakens, the warm water is not carried to the western Pacific resulting in increased Sea Surface Temperature (SST) of the east Pacific Ocean and a shift in the rainfall and Walker circulation pattern. Drought occurs over the western Pacific seriously affecting the Indian and Australian monsoon system. This situation is termed as El Niño. La Niña is the enhancement of normal conditions. That is, when the trade winds are enhanced there will be an increment in the amount of rainfall received over the Indian subcontinent and also in Australia.

Generally, there exists a negative correlation between El Niño and Indian monsoon rainfall with a substantial reduction in the annual rainfall received. All parts of the country may not be experiencing a decrease in rainfall due to this phenomenon. The recent decades have witnessed a weakening of this inverse relationship between El Niño and monsoon (Kumar et al., 1999).

India witnessed several drought years as a result of El Niño though there were years that brought drought which was not caused by El Niño. This shed light into another phenomenon called the Indian Ocean Dipole (IOD). The positive phase of IOD is marked by warmer than normal SST over the

west Indian Ocean and cooler than normal SST over the east Indian Ocean. The former brings intense rainfall to the country while the latter reduces rainfall. IOD has the potential to cause normal monsoon for India under conditions of El Niño. However, it is noted that the number of extreme El Niño years under the global warming period is likely to increase substantially (Cai et al., 2014). Three such events had occurred so far- 1982/1983, 1997/1998, 2015/2016 extreme El Niño. Each extreme El Niño was unique in their characteristics and their effects on Indian monsoon rainfall were different. It is therefore important to study the serious repercussions of the extreme El Niño years.

The objective of this study is to find out how extreme ENSO years modulate the Indian monsoon. Initially the ENSO-monsoon relationship is examined and then, the evolution of this relationship over time has been studied. Finally, the extreme ENSO years are identified and how it could affect the rainfall pattern over India is considered.

CHAPTER 2

REVIEW OF LITERATURE

2.1 INDIAN MONSOON – IMPORTANCE AND VARIABILITY

The southwest monsoon rainfall brings about 78% of the annual rainfall over the country (Roxy and Chaitra 2018). The Indian summer monsoon extends from 1 June to 30 September but exhibits year to year variations (Xavier *et al*., 2007). At the time of northeast monsoon rainfall from October to December, winds blow in the north east direction from the Indian landmass to the Indian Ocean. The north Atlantic and extratropical SST pattern along with central Pacific El Niño influence the variability of northeast monsoon rainfall (Nair *et al.,* 2018).

Except for southeast India, the main rainy season for most parts of the country is the southwest monsoon (Varikoden *et al*., 2013). The highest amount of rainfall is received by the Western Ghats and northeast India (Kishore *et al*., 2015). The Indian summer monsoon is a part of the Asian monsoon and exhibits a wide range of variability. A significant part of this variability is played by the active and break spells of monsoon which bring about excess and reduced rainfall respectively (Rajeevan *et al.,* 2010). The interannual variability of the monsoon has a great impact on the Indian economy as well as the agriculture sector which is a prominent contributor to the GDP of the country (Rajeevan and Pai 2007).

Ocean warming has its impact on the monsoon variability. Arabian sea warming reduces the monsoon precipitation over India except northeast, south central and west India due to changes in convective precipitation but the extreme rainfall events increase. The warming causes an increase in rainfall at the time of onset and then the response reverses (Mishra *et al*., 2020). The increased greenhouse gas concentration and the resultant global warming has led to an increase in the frequency and intensity of extreme rainfall events (Rajeevan *et al.,* 2008).

The year 2017 brought extreme rainfall event to the country during the southwest monsoon. The spread and frequency of the extremes were particularly high over the central, southcentral, northwest and northeast regions. The presence of convective cloud band and low-level cyclonic disturbances were found in southcentral and central India. A weak La Niña in the east Pacific coupled with a positive IOD event in the Indian Ocean favoured the occurrence of extreme rainfall event. The intensification of ascending branch of zonal circulation over central India contributed to a greater number of extremes events here (Suthinkumar *et al.,* 2019).

A strong monsoon season has the features like lowered pressure system, warm sea surface temperatures and higher precipitation to the west of the South Pacific Convergence Zone (Meehl *et al*., 1986). The frequency of extreme rainfall events shows an increasing trend over India during the south west monsoon. This is true at the time of onset and active phase during June and July respectively (Pattanaik and Rajeevan 2010).

Central and north India exhibit a reduction in the frequency of heavy rainfall whereas peninsular India, eastern parts and north east India shows an increase in the amount of rainfall. There is an increase in the number of wet days for the desert regions of the country. The last two decades also witnessed an increased possible risk of flood in eastern coast, West Bengal, east Uttar Pradesh, Gujarat and Konkan coast (Guhathakurta *et al*., 2011). Parts of east India showed a reduction in seasonal rainfall during the period 1901 to 1958 due to the decreased frequency of low and medium intensity rainfall events (Barde *et al*., 2020).

The 1.2 ˚C increase in SST over the west Indian ocean leads to a change in the land- sea thermal gradient, altering the strength of monsoon circulation patterns and the flow of moisture rich winds towards the South Asia. Enhanced convection in the Indian ocean and subsidence over the landmass resulted in reduced rainfall over central-east and northern regions of India (Roxy *et al*., 2015). From 1950 to 2015 the central India experienced a 75% increase in the extreme rainfall events even though the mean monsoon rainfall

shows a declining trend. The westerlies transport the moisture from north west Arabian sea which converge over the central India leading to widespread rainfall (Roxy *et al*., 2017).

The Western Ghats region which lies parallel to the west coast receives high amount of rainfall. An increase in the summer monsoon rainfall was observed in the northern part of the Western Ghats and a reduction in the south. This is due the enhanced rise of SST over north Arabian sea and the north Indian tropospheric temperatures which has resulted in a shift of low-level jet streams (LLJ) to the north from 10 ˚N to 15 ˚N (Varikoden *et al*., 2019).

The amount of rainfall received and the variability associated with it is high for northeast India. The extreme rainfall during the southwest monsoon is caused by the high strength of the southerly component of the low-level winds from Bay of Bengal along with convergence at 850 hPa which produce an updraft (Varikoden *et al*., 2020).

The Indian monsoon is also influenced by the African orography and it was found that the precipitation and low-level jet over India increase in the absence of the African orography. The precipitation over Bay of Bengal increases and hence advection enhances which causes an increase in rainfall. However, if the mountains over the entire globe is removed precipitation reduces and there is a delay in onset due to the intrusion of midlatitude dry air in the absence of Himalayas (Chakraborty 2002).

A decreasing trend in the seasonal mean of summer monsoon is observed over east India while it is increasing over the western parts of the country. The rising low and moderate rainfall events over central, north and northwest India is due the increased moisture transport over the Arabian sea. On the other hand, east and north east India experience a reduction in the low and moderate rainfall events due the decreased moisture transport over Bay of Bengal (Konwar and Parekh 2012).

Aerosols can also influence the variability of rainfall over India (Handler 1986; Gautham *et al*., 2009). During the pre-monsoon period increased precipitation occurs in northern India and over the Tibetan Plateau due to the black carbon aerosols and consequent weakened latitudinal SST gradient. The reduced trend in summer monsoon precipitation over India is likely to be the effect of these aerosols (Meehl *et al.,* 2008).

2.2 GLOBAL PHENOMENA AFFECTING MONSOON

The Indian Summer Monsoon Rainfall (ISMR) is affected by several phenomena including ENSO, PDO (Pacific Decadal Oscillation), AMO (Atlantic Meridional Oscillation), IOD, and others including Eurasian snow cover, and total solar irradiance (Zheng *et al*., 2020).

A warm AMO phase is characterised by warm SST anomalies over North Atlantic and cold SST anomalies over South Atlantic which causes warm SST anomalies to be formed over the western Pacific. The trade winds are weakened over the eastern Pacific and results in deepening of the thermocline here. This reduces the ENSO variability and hence weakens the ENSO south Asian monsoon relationship (Chen *et al.,* 2010). The warm AMO phase also causes a delay in the monsoon withdrawal and subsequently an increase in the rainfall over India (Goswami *et al*., 2006).

The ocean- atmospheric coupled phenomenon that takes place in the tropical Atlantic Ocean during boreal summer monsoon is termed as the Atlantic Zonal Mode (AZM). An inverse relationship exists between AZM and the Indian monsoon which means that a warm phase can weaken the monsoon and vice versa. The inverse relationship was found to be strengthened in the recent decades due to the increased interannual variability of SST pattern over east Atlantic Ocean which causes a greater number of AZM events. This further enhances the Kelvin wave response in the Indian Ocean which leads to convergence/divergence of moisture over the Indian landmass and results in the strengthening of inverse relationship (Sabeerali *et al.,* 2019)

PDO has a significant role in the monsoon variability over India. The dry monsoon of 1972, 1968, 1918 was the result when warm phase of ENSO occurred in conjunction with then cold phase of PDO and the years 1988, 1942, 1933, 1916 witnessed wet monsoon when cold phase of ENSO cooccurred with warm PDO (Krishnan and Sugi 2003). There exists a strong out of phase relationship between the monsoon depressions over Bay of Bengal and PDO. The warm phase of the PDO causes warming of the west equatorial Indian Ocean and thereby cause weakening of the moisture transport towards Bay of Bengal and therefore cause a reduction in the monsoon depressions over Bay of Bengal (Vishnu *et al*., 2018).

An inverse relationship exists between Eurasian snow cover and the Indian summer monsoon rainfall. A high winter snow cover of Eurasia can decrease the summer rainfall of the following year (Vernekar *et al.,* 1995) and this relationship was found to be valid only with the western Eurasia (Bamzai and Shukla 1999).

ENSO and IOD are the two major drivers that can affect the inter annual variability of the ISMR (Krishnaswamy *et al*., 2015). The intensity of IOD and El Niño and La Niña events can influence the anomalies associated with the summer monsoon rainfall (Ashok *et al*., 2001). The dipole mode in the Indian Ocean accounts for about 12% of the SST variability and found to be independent of the ENSO events. Indian Ocean Dipole is characterised by abnormal low SST over the Sumatra region and high SST over western Indian Ocean (Saji *et al*., 1999; Webster *et al.,* 1999). Monsoon trough areas and parts of west coast are the regions where IOD has its greatest impacts (Ashok and Saji 2007).

A positive IOD event can lessen the influence of El Niño and can lead to normal rainfall in the Indian subcontinent whereas the co-occurrence of a negative IOD with La Niña leads to reduced rainfall (Ashok *et al.,* 2004). Under greenhouse warming condition there is a redistribution of rainfall over the Indian Ocean and the relationship between IOD and Asian summer monsoon rainfall is growing rapidly (Abram *et al.,* 2008). Ajayamohan and

Rao (2009) suggested that the extreme rainfall events over central India is related to the IOD events. The cool SST anomalies over the south equatorial Indian Ocean is responsible for the extreme rainfall here.

The rainfall of central Indian region is generally normal during the IOD years. In contrast the year 2008 witnessed a below normal rainfall despite of a positive IOD event because of the strong warming over subtropical Indian Ocean which created a positive IOD as well as warming over the tropical Indian Ocean (Rao *et al*., 2010).

The relationship between ENSO and IOD shows a weakening trend in the recent decades. This is attributed to the different spatial pattern created in ENSO evolution at the time of boreal spring and summer seasons (Ham *et al.,* 2017). The dominant mode of the Indian Ocean shows uniform cooling or warming of the SST which has a greater influence on the monsoon than the Indian Ocean Dipole. The southern Indian Ocean SST has more impact on the Asian summer monsoon than the northern part.

Anil et al., (2016) studied the different flavours of IOD and its relation with summer monsoon rainfall pattern. During early IOD (EIOD) and prolonged IOD years (PIOD) the sea surface temperature anomaly over Arabian sea is positive and results in stronger evaporation and cross equatorial flow. This causes increased monsoon rainfall over India. The number of break days are also considerably less during this time. But normal IOD years have comparatively more break days.

2.3 EL NIÑO SOUTHERN OSCILLATION

The natural variabilities in the world climate are largely influenced by the tropical oceans due to the coupled ocean- atmospheric phenomena generated here. El Niño Southern Oscillation is one such typical phenomena that develop in the tropical Pacific Ocean on an inter annual time scale (Yamagata *et al*., 2004). The periodic warming and cooling caused by ENSO

largely influence the water cycle over the tropical region (Allan and Soden 2008).

El Niño is characterized by warmer than normal SST over central and east equatorial Pacific Ocean whereas La Niña is marked by colder than normal sea surface temperatures. Southern Oscillation is defined as the fluctuation between this El Niño and La Niña events that complement each other (Philander 1985). The Southern Oscillation is an important feature to be taken into consideration since it can affect the seasonal rainfall over Indian subcontinent. The large changes associated with the rainfall are related to changes in the Southern Oscillation Index values (Pant and Parthasarathy 1981).

The El Niño events are marked by a reduction in the rainfall over the Indian subcontinent which is followed by the occurrence of droughts. The changes in the zonal walker circulation during El Niño cause anomalous subsidence over the Indian landmass thereby supressing the monsoon circulation (Ummenhofer *et al*., 2011). El Niño conditions were responsible for drought conditions during ISMR and 72% of the drought years occurred under the influence of Pacific Ocean. The entire west coastal belts, monsoon zone and eastern regions were affected due the El Niño related droughts. El Niño events are also conducive for severe droughts over Western Ghats (Varikoden *et al*., 2015). The onset of monsoon over central India is affected by the pre monsoon surface pressure anomalies over north Arabian Sea and Western Asia which is a manifestation of ENSO and PDO. The negative surface pressure anomaly over Western Asia results in an early onset over central India (Chakraborty and Agrawal 2017).

From 1901–2012 the western Indian ocean had been experiencing an anomalous rise in the SST compared to the central east Indian Ocean. The irregularity in the ENSO teleconnection causes the El Niño events to induce this abnormal warming over the west Indian ocean but La Niña does not show the opposite impact (Roxy *et al*., 2014).

ENSO and IOD can have a great influence on the planetary waves in Bay of Bengal. At the time of weak El Niño, the second downwelling Kelvin waves are weakened whereas these are strengthened during strong El Niño years (Sreenivas *et al.,* 2012). A warm (cold) ENSO phase can increase (decrease) the winter time precipitation over northwest India. Enhanced western disturbances due to lower geopotential height and strong north easterly flow were observed during warm ENSO phase (Dimri 2013).

Based on the SST anomaly over the equatorial Pacific Ocean, two types of El Niño events are identified warm pool El Niño (WP) and cold tongue (CT) El Niño. The large SST anomalies over Niño 3 region results in CT El Niño while WP El Niño has large SST anomalies over Niño 4 region (Kug *et al*., 2009).

ENSO in the tropical Pacific is of two types- an eastern-Pacific (EP) type and a central-Pacific (CP) type. The EP type of ENSO is found to have its SST anomaly center located in the eastern equatorial Pacific and shows a strong teleconnection with the tropical Indian Ocean. In contrast, the CP type of ENSO has its SST anomalies confined in the central Pacific and has a stronger teleconnection with the southern Indian Ocean (Kao and Yu 2009). The CP type plays a great role in producing droughts over India (Fan *et al.,* 2017).

The SST pattern of the EP El Niño is greatly influenced by the thermocline feedback while the CP El Niño is affected by the zonal advection near the edge of the warm pool (Capotondi *et al*., 2015). The initial state of the thermocline plays an important role in the development of EP and CP type El Niño. A thermocline which is deeper in the eastern Pacific but which is shallower in the western Pacific favours El Niño in the Niño 1+2 area whereas a shallow thermocline in the east and a deeper one in the west and central pacific is conducive for a CP one (Capotondi and Sardeshmukh 2015).

The frequency of CP El Niño has increased compared to the EP type. The CP events have doubled in the recent period after 1980 and the number

of events has rose to 9 in 30 years from the previous 3.5. On contrary the number of EP events are relatively low at about 2 events in 30 years (Freund *et al.,* 2019). It is also important to note that the intensity of the CP El Niño events had been increasing for the past three decades at the rate of 0.2 C per decade. The EP events on the other hand exhibits a cooling trend (Lee and McPhaden 2010).

The El Niño events in which warming is concentrated over central equatorial Pacific is capable of producing more droughts in India than the ones caused by eastern Pacific El Niño (Kumar *et al*., 2006). The EP type of El Niño is found to have a strong positive relationship with the winter precipitation of north and central India. Warm SST anomaly over the western Indian Ocean during winter in response to the El Niño cause the downward motion of the Hadley cell over central India. This sinking motion results in the enhancement and shift of subtropical westerly jet stream to north India. The subtropical westerly jet stream causes barotropic and baroclinic instability which intensifies the western disturbances and hence excess precipitation occurs over north and central India (Yadav *et al.,* 2013)

In 2004 an El Niño event occurred and was different from the conventional one. This was marked by warming in the central Pacific flanked by cold SST over the eastern and western Pacific. This phenomenon was termed El Niño Modoki which means a similar but a different thing. The temperature and rainfall pattern of the world are affected by El Niño Modoki. A reversal of this phenomenon is called La Niña Modoki characterised by colder central Pacific SST and warmer SST on either side such as the one happened in 1998 (Ashok et al., 2007). El Niño Modoki exhibits different climatic pattern compared to the canonical El Niño due to the formation of twin Walker circulation cells in the tropical Pacific (Weng *et al.,* 2007).

During the winter monsoon of Indian subcontinent, the warm pool El Niño brings ambient amount of rainfall over the western Himalayas and the north western parts of India but reduced rainfall over the foothills of Himalayas and the central India (Dimri 2017). The summer monsoon rainfall

has different characteristics during wet and dry years which may or may not be related to ENSO. During normal El Niño years which brought normal rainfall to the country the rainfall anomaly was particularly high over in the northern part of the west coastal regions and uniformly distributed over central India. El Niño drought years caused minimum rainfall over Indian peninsula and north India (Varikoden and Preethi 2013).

An extreme El Niño is defined as an event in which there is a massive reorganization in the convection pattern and the Niño 3 rainfall exceeds 5mm/day. It is also marked by an eastward extension of the warm pool and the subsequent coverage of the entire equatorial Pacific Ocean. It is proposed that in the climate change period, the frequency of extreme El Niño events doubles (Cai *et al*., 2014).

Marjani *et al*., (2019) argued that there is no increase in the number of extreme ENSO events in the second half of the twenty first century under the global warming scenario. The extreme El Niño events show a decrease in number while the extreme La Niña events remain steady.

The ISMR variability is also linked to the different decay phases of El Niño. There is excess rainfall at the time of early decay phase, normal at the time of mid-summer decay and deficit during no summer decay (Chowdary *et al*., 2016). The break phase associated with monsoon are two to three times more at the time of El Niño developing phase summer and it lasts for 10 to 15 days. The opposite is true for El Niño decay years (Pillai and Chowdary 2016).

The Indian monsoon variability can also influence the ENSO conditions. A weak monsoon can enhance the warm event in the equatorial Pacific Ocean through surface zonal wind stress anomalies but a strong monsoon can reduce this warming. It is also worthy to note that the monsoon variability cannot influence a cold event (Wu and Kirtman 2003). El Niño can affect the onset of Somali Jet by inducing a delay of 2 days compared to La Niña. The 1997 extreme El Niño caused a very late onset of the Somali Jet

and also a reduction in its strength. As a result, the rainfall over west coast of India had reduced substantially. On the other hand, a greater strength of the Somali Jet can bring about excess rainfall (Halpern and Woiceshyn 2001).

India witnessed a severe drought in the year 2009 with 29% reduction in the June – September seasonal rainfall. The warming in the central Pacific was responsible for this reduction in rainfall over the whole of the Indian Ocean, Indian subcontinent and over the eastern Pacific. This El Niño Modoki condition caused a shift in the walker circulation and subsidence over Indian landmass. Central Pacific and northwest Pacific experienced anomalously high rainfall (Ratnam *et al.,* 2010).

The inverse relationship between ENSO and Indian monsoon shows a weakening trend in the recent decade after 1980's. Surface warming over Eurasia exceeds the Indian ocean warming and results in increased land-sea thermal gradient which could bring about normal rainfall conditions over India despite a strong El Niño event. Another reason is thought to be the south-eastward shift of the walker circulation which could reduce the subsidence over India and usual rainfall pattern prevails here (Kumar *et al.,* 1999). Chang *et al.,* (2001) reported that the weakening relationship is due to the strengthening and poleward shift of the jet streams over North Atlantic.

However, the relationship between ENSO and northeast monsoon rainfall over the southern peninsular India has increased. The rainfall of the regions that lie in the windward side of Western Ghats shows greater correlation with ENSO due to the enhancement of low-level circulation during northeast monsoon which increases the orographic component of rainfall (Zubair and Ropelewski 2006). Sarkal *et al*., (2004) argues that the relationship between monsoon rainfall and ENSO has increased recently. The effect of ENSO is felt only when the bipolarity in the Indian Ocean is low but the recent years had witnessed a strong and consistent bipolarity. This has caused an increased local dynamics and circulation patterns which has nullified the effect of ENSO on rainfall over India.

The changes in the north Pacific SST also plays an important role in the weakening of the ENSO-monsoon relationship. This leads to changes in the atmospheric circulation over east Asia and western Pacific (Kinter III *et al*., 2002). The recent period also witnessed a change in the mean state of the wind flow over north western Pacific which showed a cyclonic intensification at the same time. This weakens the anticyclonic flow south east of Japan. Also, the cross-equatorial circulation in the tropical Indian Ocean has strengthened due to decadal variability of the Mascarene High. These have also resulted in the weakening of the teleconnection between ENSO and monsoon (Feba *et al*., 2019).

Before 1970s the relationship between rainfall and ENSO was strong in central and northwest India during the late summer season but weakened later. Northeast India exhibited a strong relationship in the early summer after 1970 (Kawamura 2005).

Twenty first century witnessed its first El Niño in the year 2001/2002. Though the event was moderate Indonesia, northern and eastern Australia, and north eastern South America experienced drier than normal conditions and wetter than normal conditions prevailed over central equatorial Pacific. The Indian summer monsoon rainfall was reduced drastically during the summer of 2002 (McPhaden 2004). Increased frequency of high temperature extremes is observed at the time of monsoon and post monsoon season in response to El Niño while this frequency is comparatively lower in the pre monsoon season. The opposite is true for La Niña condition (Revadekar *et al.,* 2009).

The frequency of extreme La Niña events are projected to increase further under greenhouse warming conditions. The increased frequency of extreme El Niño along with rising upper ocean vertical temperature gradient and warming of the maritime continent are favourable for extreme La Niña events to occur repeatedly (Cai *et al.,* 2015). The 2015/2016 was among the strongest El Niño events dating back to 1950. It was characterised by warmer

west-central Pacific surface and subsurface temperature anomalies but for the eastern Pacific, it was comparatively warmer (L'Heureux *et al*., 2017)

Though El Niño was extreme in 1997/1998 and 2015/2016, the events were different from each other. The former one was EP (Eastern Pacific) type while the latter included both EP and CP (Central Pacific) (Paek *et al.,* 2017). It is worthy to note that this difference in the SST anomalies for the two was the reason for a strong positive IOD event which cooccurred with the 1997/1998 extreme El Niño but the positive IOD was weak at the time of 2015/2016 extreme El Niño. There were two walker cells for the 1997 event in which one ascending branch was over the east equatorial Pacific and the other over western tropical Indian Ocean. On the other hand, the 2015 event rising branch was over the central tropical Pacific (Liu *et al*., 2017). The atmospheric component of the IOD is referred as the Equatorial Indian Ocean Oscillation (EQUINOO) which can influence the summer monsoon rainfall anomalies by enhancement (suppression) of atmospheric convection over the western (eastern) Indian ocean (Gadgil *et al*., 2004). Extreme IOD can influence the onset of El Niño through the east west Walker circulation. It can have impact on El Niño onset predictability and can lead to the formation of El Niño Modoki in certain years such as the happened in 1994 (Luo *et al*., 2010).

The relation between monsoon rainfall and IOD exists in the summer and autumn season but with that of ENSO extends for a long period of time and is stronger (Cherchi and Navarra 2013). A normal or high rainfall is expected during the summer monsoon season even though there exists an El Niño event because of the presence of negative zonal wind anomalies over the equatorial Indian Ocean (Ihara et al., 2007). The northeast monsoon which is the main rainfall season for Tamil Nadu is found to have a positive correlation with El Niño. The moisture transport and precipitation are strengthened at the time of northeast monsoon during El Niño years. The opposite also holds true (Geethalakshmi *et al*., 2009).

In 1982 and 1987 the monsoon rainfall was deficient in the country due to the impact of strong El Niño and the subsequent modification of the Walker circulation. But in 1997 when an intense El Niño happened there was above normal rainfall due to the fact that the change in the Walker circulation produced a modification of the local Hadley circulation over Indian Ocean and the Maritime continent and the tropical convergence zone was located to the north over Asian summer monsoon domain (Slingo and Annamalai 2000).

The westerly wind events (WWE) have the capability to trigger a strong El Niño event in the tropical Pacific Ocean. This results in the propagation of a downwelling kelvin wave to the east Pacific which creates SST anomalies in the central and east Pacific and causes the initial warming. Hence the east-west thermal gradient is decreased and weakens the trade winds and also the equatorial upwelling. These can increase the initial SST anomaly (Lengaigne *et al*., 2004).

The 2015 extreme El Niño produced intense north east monsoon rainfall. The contrasting SST gradient between western Indian Ocean and western Pacific Ocean caused strong north easterly wind anomalies which carry moisture sufficient for an intense northeast monsoon rainfall (Singh *et al.,* 2019). Also, the 2015 El Niño brought heavy rainfall over southeast peninsular India at the time of north east monsoon rainfall. The major cause of this was the presence of strong easterly wave over southeast peninsular India (Sanap *et al.,* 2019).

2.4 IMPACTS OF ENSO

ENSO can cause interannual temperature and precipitation changes world-wide which in turn affect the energy and water use, ecosystem dynamics and human health (Cobb *et al*., 2013). The extreme El Niño event of 2015/2016 has critically affected the population of the endangered leatherback turtles residing in the east Pacific region by declining their reproductive rate by 19% (Tomillo *et al*., 2020). The distribution of anchovy fish population has become more coastal instead of being widely distributed

over the entire Peruvian coast (Ñiquen and Bouchon 2004). The variabilities related to the frequency of extreme rainfall at the time of northeast monsoon is strongly influenced by El Niño Southern Oscillation events and the onset of El Niño is followed by an increase in the number of extreme event (Revadekar and Kulkarni 2008).

The impacts caused by ENSO include disruption of the global circulation patterns, drought, flood, extreme weather events and marine ecosystem disturbance (McPhaden 2015). La Niña can have impact on African rainfall. The most consistent relationship is with the southwest African rainfall with a general increase in the rainfall in the initial few months post La Niña (Nicholson and Selato 2000). El Niño causes a decrease in the primary production of organic material due to the reduction in the amount of nutrients which are transported to the surface and disrupts the food chain. This in turn decreases the growth and reproductive success of zooplanktons, fishes, birds, marine mammals (Barber *et al.,* 1983).

The 1982/1983 extreme El Niño caused a deterioration of coral reefs in the Java sea. The increased SST from the warming resulted in the bleaching of corals (Brown 1990). Due to the increased warming of the tropical Indian Ocean and higher number of extreme El Niño events the Indian subcontinent is likely to experience higher number of heat waves in the future (Rohini 2016).

CHAPTER 3

MATERIALS AND METHODS

The following datasets were used for the analysis:

IMD monthly and daily gridded rainfall data with a resolution of 0.25°×°0.25 lat./long were used for the analysis (Pai *et al*., 2015).

The SST data used is the Hadley Centre Sea Ice and Sea Surface Temperature data set (HadISST) obtained from the Met Office Hadley Centre observations datasets. It contains monthly global gridded SST and sea ice concentration dataset from 1871 onwards on a 1degree latitude-longitude grid (Rayner *et al*., 2003).

Monthly vertical velocity values are obtained from NCEP/NCAR Reanalysis Version 1. It has a spatial coverage of 2.5-degree x 2.5-degree global grids. The data is available from 1948 to 2020 (Kalnay *et al*., 1996). NOAA-CIRES-DOE Twentieth Century Reanalysis (V3) is used for retrieving the past data which has monthly vertical velocity values from 1836 to 2015. It has got a spatial coverage of 1.0-degree latitude x 1.0-degree longitude global grid. Both the data were merged to obtain monthly values of the study period from 1901 to 2018.

Monthly geopotential values as well as monthly values of u-wind and v-wind pressure levels were obtained from NOAA-CIRES-DOE Twentieth Century Reanalysis (V3) which has got a resolution of 1.0-degree latitude x 1.0-degree longitude global grid. The data is available from 1836 to 2015.

Nino 3.4 Index was used to isolate the El Niño and La Niña years. Niño 3.4 covers the region (5 ° N-5 ° S, 170 ° W-120 ° W). The Niño 3.4 anomalies represents the average equatorial SSTs across the Pacific from about the dateline to the South American coast. The Niño 3.4 index is calculated by using a 5-month running mean, and El Niño or La Niña events are defined when the Niño 3.4 SSTs exceed +/- 0.4C for a period of six months or more

(climate prediction centre, NOAA). SST anomaly during the southwest monsoon season (June to September) is used to calculate the index for a period of 118 years from 1901 to 2018.

METHODS

Timeseries Analysis

In a timeseries a set of observations or datapoints are taken at the specified time. On the X axis we have the time which is divided into equal intervals and on the Y axis is the magnitude of the data. Timeseries forecasting could be used to predict the future values based on the past observed values. Timeseries analysis is carried out by the detrended SST anomaly of Nino 3.4 and rainfall anomaly to study their evolution with time.

Correlation Analysis

Correlation analysis is a statistical method which explains the strength of relationship between two variables or it can be said as the measurement of similarity between two signals. A strong correlation indicates close association between the variables and a low correlation indicates weak association. Correlation coefficient represents the numerical measurement of this strength and the value lies between -1 and 1. A negative correlation shows inverse relationship between the variables and a positive correlation means that as one variable increases the other also increases. 0 correlation coefficient implies that there is no correlation between the variables. Correlation analysis is carried out between summer monsoon rainfall anomaly and SST anomaly of the Nino 3.4 region during JJAS (June, July, August, September) for 118 years from 1901 to 2018 to analyse the relationship between them.

The equation of the correlation function is given by:

$$r_{xy} = \frac{\sum(x_i - \bar{x})(y_i - \bar{y})}{\sqrt{\sum(x_i - \bar{x})^2 \Sigma(y_i - \bar{y})^2}}$$

Where:

r_{xy} – the correlation coefficient of the linear relationship between the variables x and y

x_i – the values of the x variable in a sample

$\bar{x}$ - the mean of the values of the x variable

y_i – the values of the y variable in a sample

$\bar{y}$ - the mean of the values of the y variable

Cross Correlation

Cross correlation represents measurement of similarity between two different signals or series. Here the similarity is measured between a signal and shifted version of another signal. Consider two series x(i) and y(i) where i=0,1,2...N-1. The cross-correlation r at delay d is defined as

$$r = \frac{\sum_i [(x(i)-mx)*(y(i-d)-my)]}{\sqrt{\sum_i (x(i)-mx)^2}\sqrt{\sum_i (y(i-d)-my)^2}}$$

Where:

mx and my are the means of the corresponding series

Empirical Orthogonal Function (EOF) Analysis

EOF analysis is used to study the pattern or spatial mode of variability and how it evolves over time. It is also known as the principal component analysis. In EOF a field is divided into mathematically orthogonal modes which represent atmospheric and oceanographic modes. The EOFs are found by computing the eigenvalues and eigenvectors of a spatially weighted anomaly covariance matrix of a field. Generally, the spatial weights are the cos(latitude) or, better for EOF analysis, the square root(cos(latitude)). The derived eigenvalues provide a measure of the percent variance explained by each mode. The time series of each mode obtained from principle components are determined by projecting the derived eigenvectors onto the spatially

weighted anomalies. This results in the amplitude of each mode over the period of record.

EOF patterns can reveal underlying teleconnections that simple correlations cannot reveal. EOF analysis is carried out for ISMR for the period 1901 to 2018 to detect the major causes of monsoon variability. From the analysis a major cause and a minor cause of variability will be obtained.

Wavelet Analysis

The variation of power within a timeseries can be analysed using wavelet analysis. In this method, the timeseries is decomposed into time frequency space and one could interpret the dominant mode of variability and how those modes vary in time. Wavelet analysis is useful in the study of the variations in the frequency of occurrence and amplitude of ENSO events (Torrence and Compo 1998).

A continuous wavelet transform is given by:

$$W_n(S) = \sum_{n'=0}^{N-1} x_{n'} \sqrt{\frac{\delta t}{s}} \psi_0 * \left[\frac{(n'-n)\delta t}{S}\right]$$

Where:

Xn is a time series with equal time spacing δt and n= 0…. N-1

(*) indicates the complex conjugate

Wavelet analysis is carried out for north, central and south India rainfall from 1901 to 2018. From the corresponding time series, it is possible to find

the periodicity associated with each, whether it is a year to year, decadal or multi-decadal variability.

Power Spectrum

Power spectrum gives an idea of how the intensity of a time varying signal is distributed in the frequency domain or how much of a signal is at frequency ω. For a given power spectral density S, the bandlimited power spectrum is given by:

$$\frac{1}{\pi}\int_{w_1}^{w_2} S(\omega)\, d\omega$$

Power spectrum analysis is carried out for north, central and south India rainfall from 1901 to 2018. Power spectrum is a continuity of the wavelet analysis wherein one is able to find the timescale corresponding to the periodicity of rainfall variability.

Composite Analysis

Composite analysis involves the study of the basic structural characteristics of a climatic phenomenon. This is useful in understanding the impacts of teleconnections caused by large scale processes such as ENSO. The large number of cases of a given phenomenon is collected and is standardised which are composited together as a function. Composite analysis involves computing the composite mean.

CHAPTER 4

RESULTS AND DISCUSSION

For the study on the influence of extreme ENSO events on Indian monsoon, initially the ENSO-monsoon relationship was investigated. Secondly the evolution of ENSO-monsoon relationship was taken into consideration. Finally, the impact of extreme ENSO events on southwest monsoon rainfall was studied. The following sections are arranged accordingly.

4.1 ENSO-MONSOON RELATIONSHIP

It has been observed that there is a strong inverse association between ENSO and Indian summer monsoon rainfall (ISMR). Warm ENSO like condition is observed to be related to reduced ISMR and drought in the Indian subcontinent. In this chapter, we try to summarize the observed relationship between ENSO and Monsoon.

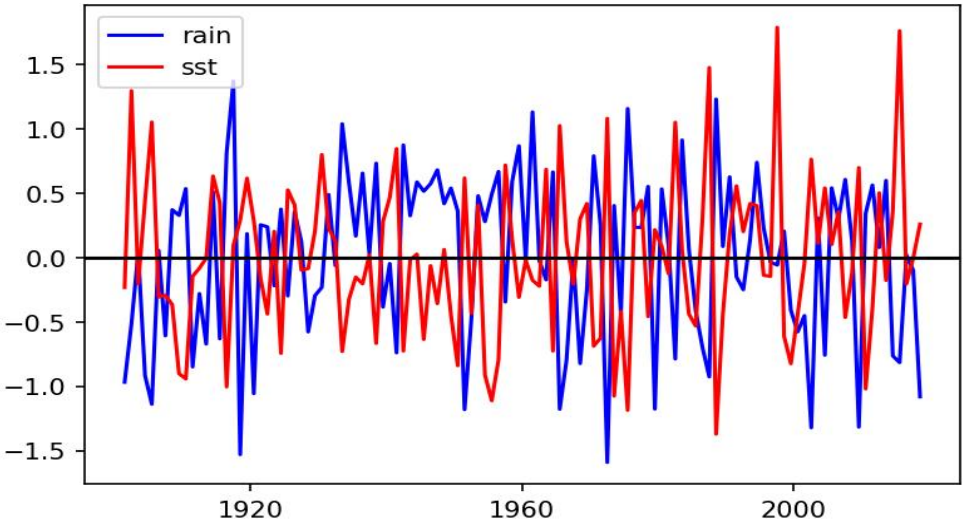

Figure 1. Correlation between ISMR and Niño 3.4 SST (JJAS monthly anomaly)

The relationship between ENSO and ISMR is studied from the timeseries plot (Figure 1) of the seasonal mean anomaly of summer monsoon rainfall and the SST(JJAS) over Niño 3.4 region (5°S–5°N, 170°W–120°W) during 1901 to 2018. A significant negative correlation (r=-0.56) between Niño3.4 and ISMR is observed. The correlation between DJF (December, January, February) Niño 3.4 SST and ISMR is found out to be 0.0536.

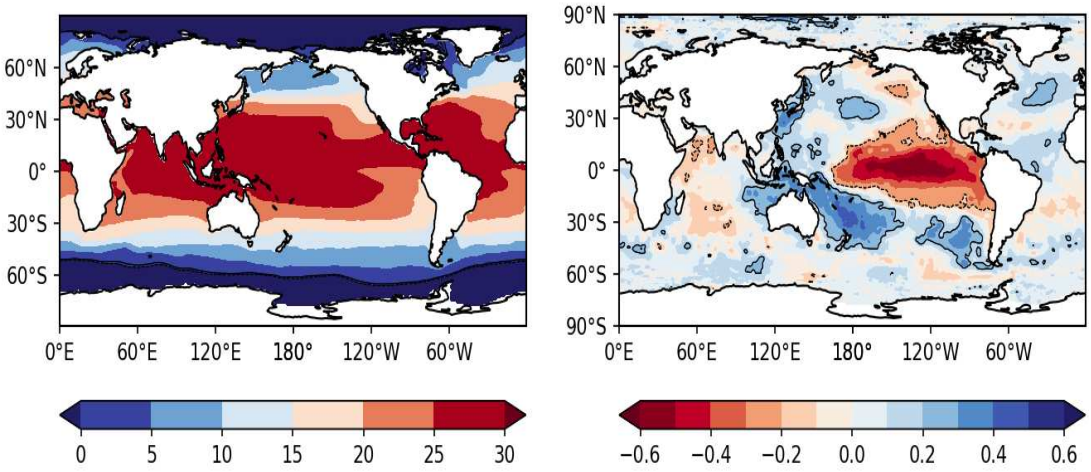

Figure2. (a) Average SST of the global oceans in °C (b) SST of the global oceans correlated with ISMR (JJAS monthly anomaly)

Figure 2(a) shows the average SST of the global oceans during JJAS from 1901 to 2018. Temperature is indicated in °C. Temperatures greater than 20°C are found in most of the world oceans. Warmest SST is observed in the western Pacific and Indian ocean during JJAS greater than >28 ˚ C. This high SST is favorable for deep convection and is the main source of south Asian summer monsoon.

Figure 2(b) gives the monthly anomaly of SST(JJAS) of the global oceans correlated with the summer monsoon rainfall of India for the period 1901 to 2018. From the figure a strong negative correlation is observed over

the east and central parts of the equatorial Pacific which is similar to the canonical ENSO SST pattern.

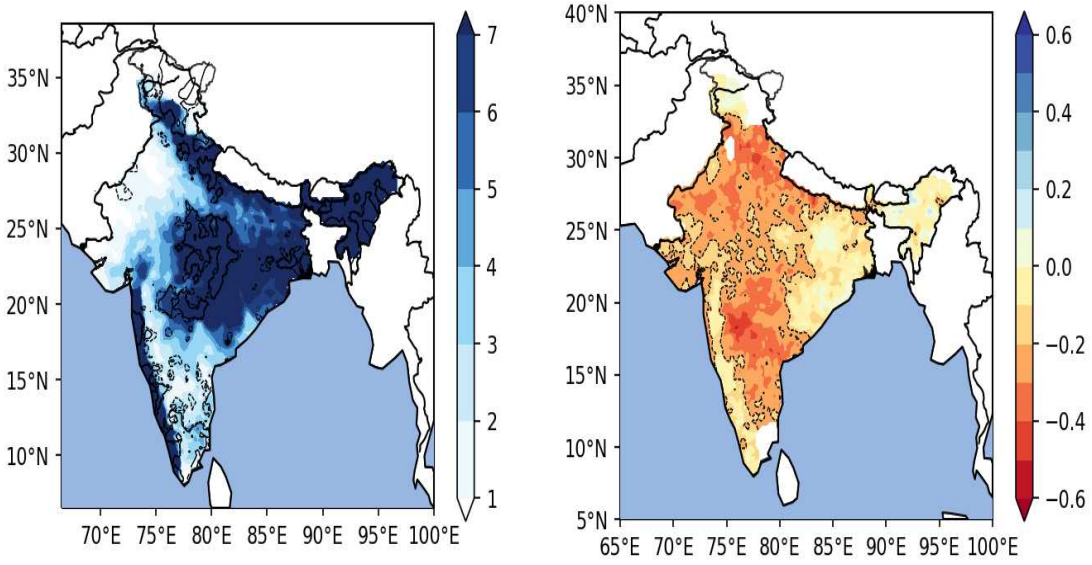

Figure 3. (a) The average of ISMR from 1901 to 2018 (b) The spatial distribution of rainfall correlated with the ENSO conditions

Figure 3(a). represents the average rainfall over India during JJAS from 1901 to 2018. The regions of Western Ghats, east India, northeast India and foothills of Himalayas are bestowed with sufficient amount of rainfall whereas south India and northwest India have reduced rainfall. Figure 3(b) shows the spatial correlation of Niño 3.4 SST(JJAS) anomaly with Indian summer monsoon rainfall anomaly (1901-2018). Overall, there is a negative correlation for most parts of India except for the Western Ghats, east India and the northeast India. Correlation coefficient with values ranging from -0.2 to -0.6 is found in south, central and parts of North India which is statistically significant at the 95% confidence level.

The Hadley cells extend from 0° to 30° latitude north and south. At the equator the air is warm and it rises. This warm air cools as it ascends and sinks at 30° latitude. The Hadley circulation shifts northward along with the Inter Tropical Convergence Zone (ITCZ) during boreal summer months in JJAS. Studies have shown that ENSO affects the Hadley circulation. During El Niño years the anomalously warm water generates stronger ascending motion of air and the descending branch would be more concentrated towards the equator. Thus El Niño leads to stronger and narrower Hadley circulation but La Niña causes weaker and widened circulation (Y. Hu *et al*., 2018). The shrinkage is associated with the equatorward movement of Hadley circulation eddies during El Niño years compared to normal years (Guo and Li 2016).

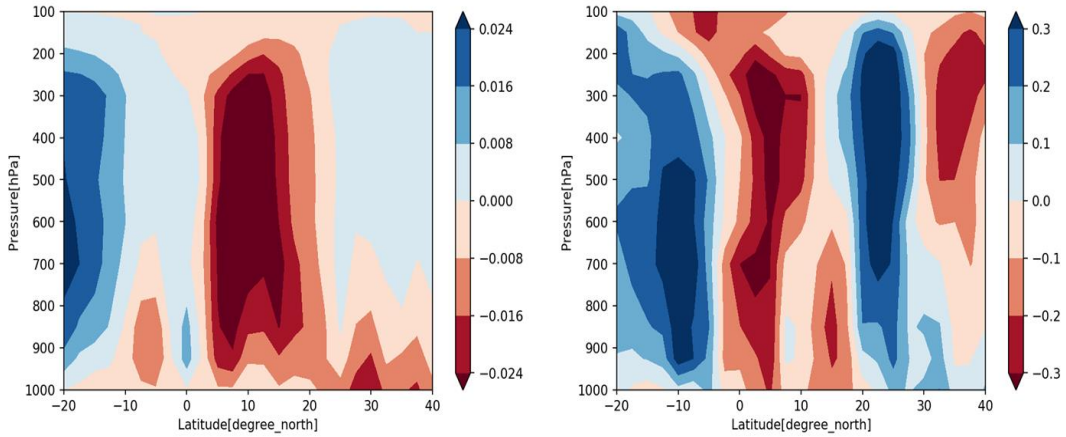

Figure 4. (a) Hadley circulation (JJAS) from 1901 to 2018 .Negative omega (Pa s1) represents upward vertical velocity (b) correlation with JJAS monthly mean anomaly of : Niño 3.4 SST

Figure 4(a). shows the average vertical velocity for the zonal mean of latitude 20°S to 40°N for the period 1901 to 2018 during JJAS. The ascending branch of the Hadley cell is confined over 5˚N to 22˚N which indicates upward motion. Figure 4(b). gives the correlation between Niño 3.4 region and vertical velocity (omega) for the zonal mean of latitude 20°S to 40°N. A

strong positive correlation is observed at 20°N to 25°N. This means that the good ISMR is accompanied by the extension of the ascending branch of the Hadley cell to further north. There is anomalous ascending motion over the equatorial region and anomalous subsidence over 20˚ N to 30˚ N. So here we can see that with the effect of Nino 3.4 SST, subsidence has occurred over the Indian landmass particularly over the northern parts which had ascending motion otherwise.

Under normal conditions as the trade winds move from east equatorial Pacific to the west warm water is carried along with them. This warm water piles up over west and the warm air rises up. After reaching certain level the air cools and descends over the east, thus completing the walker circulation. But under El Niño conditions there is a shift in the walker circulation.

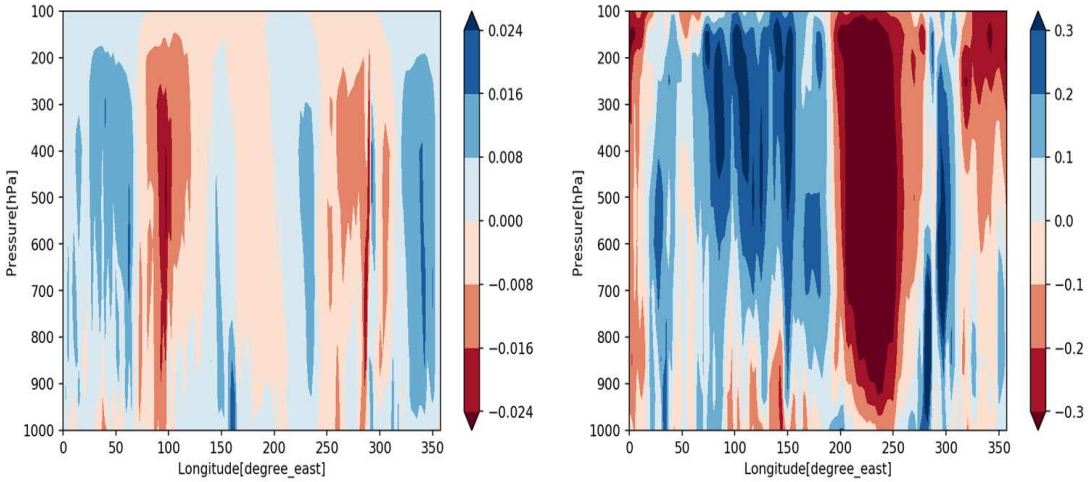

Figure 5. (a)Walker circulation (JJAS) from 1901 to 2018 (b) correlation with JJAS monthly mean anomaly of Niño 3.4 SST

Figure 5(a). shows the average vertical velocity for the meridional mean of the entire longitude from 1901 to 2018 during JJAS. There is ascending motion over eastern Indian Ocean. Figure 5(b). shows the correlation between Niño 3.4 SST monthly anomaly and the meridional mean for the entire longitude. Negative correlation can be observed at 200°E to 260°E longitude.

This implies an upward motion at eastern Pacific Ocean which resembles El Niño condition. Also, there is subsidence over eastern Indian Ocean.

This chapter signifies the relationship between ENSO and the Indian Summer Monsoon Rainfall. It was analysed through the correlation analysis between the JJAS monthly mean anomaly of rainfall and Niño 3.4 SST. The regions which are affected by the ENSO teleconnections were identified. The changes to Hadley and Walker circulations under ENSO conditions were also examined.

4.2 EVOLUTION OF ENSO-MONSOON RELATIONSHIP

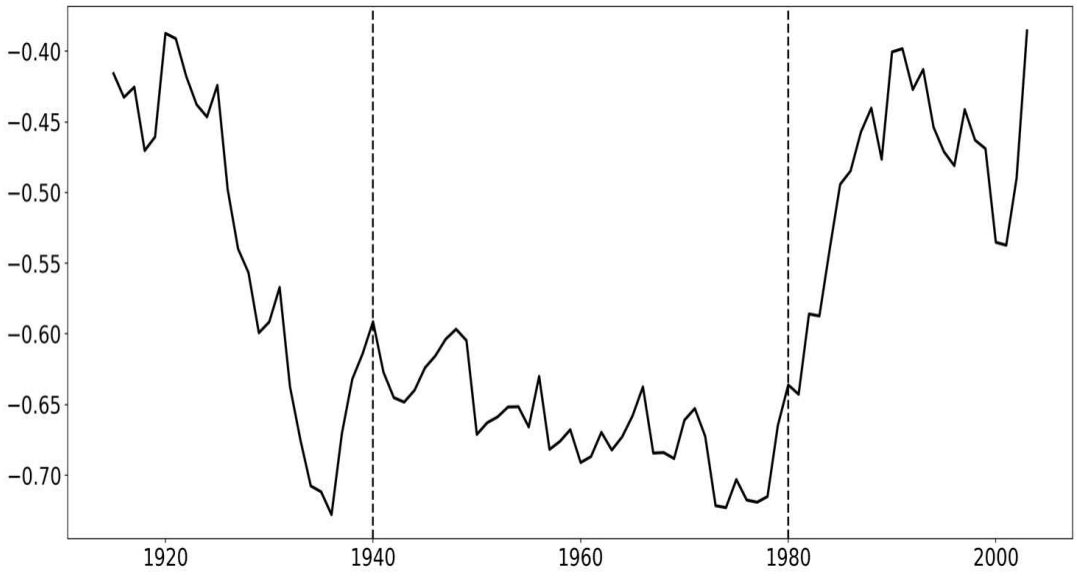

Figure 6. 30 year running correlation of the relationship between rainfall and Nino 3.4 SST anomaly during JJAS from 1901- 2018

The figure represents the 30-year running correlation of ENSO-monsoon relationship for the period 1901 to 2018. The correlation coefficient ranges from -0.40 to -0.70. From 1901 the correlation started rising and became stable for the period 1940 to 1980 with a very strong negative correlation between the values -0.6 to -0.7. Then after 1980, the correlation began to decrease. From the plot it can be observed that the ENSO-monsoon connection is not the same for the entire period monitored. A clear change can be demarcated from the figure wherein the initial period from 1901 to 1940 shows an increase in the association which became steady in the middle period from 1940 to 2018. In the recent period from 1980 to 2018 the relationship started declining from a coefficient value of -0.6 to -0.4.

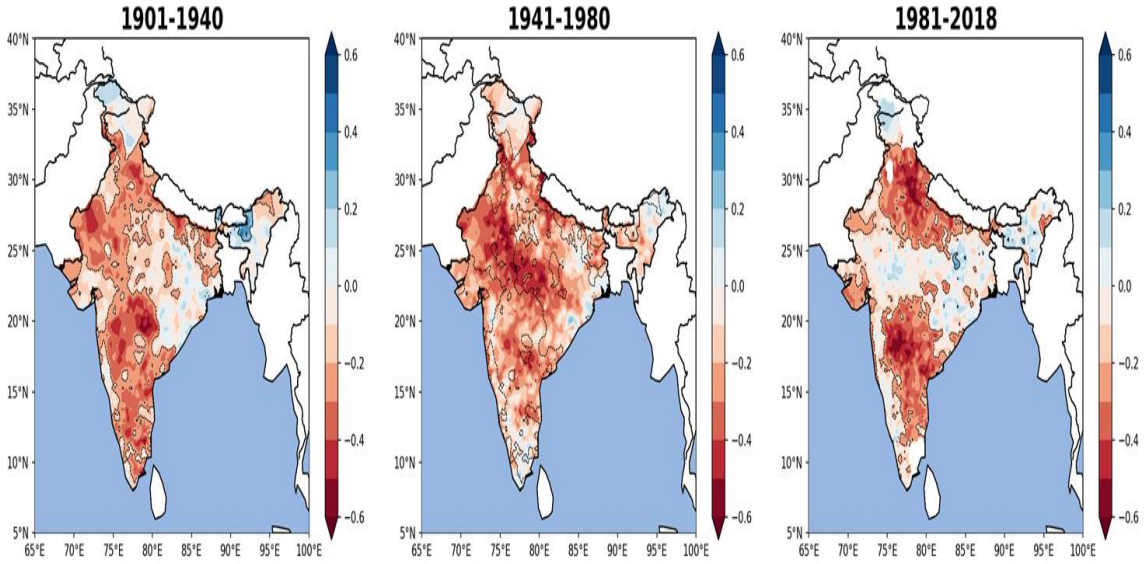

Figure 7. Spatial map of correlation between rainfall and Nino 3.4 SST anomaly for different periods

The figure shows the spatial map of the correlation between anomalies of summer monsoon rainfall and SST of the Nino 3.4 region (JJAS) for different epochs. It was observed that the ENSO-monsoon relationship varies over time. Now it can be noted that this interrelationship varies spatially also. From 1901 to 1940 the relationship was prominent over south India, parts of west and north India. In the middle period there has been a rise in the correlation covering almost the entire parts of India. But there is a drastic reduction in the correlation after 1980 in which only south and north India exhibits the association. Central India and Western Ghats are devoid of a negative interrelationship and a weak positive correlation can also be observed. Comparing all the three it can be said that the ENSO-monsoon relationship for south India is stable for all the three periods, for central India it is decreasing in the recent period and for north India there is a gradual increase in the relationship from 1901 to 2018.

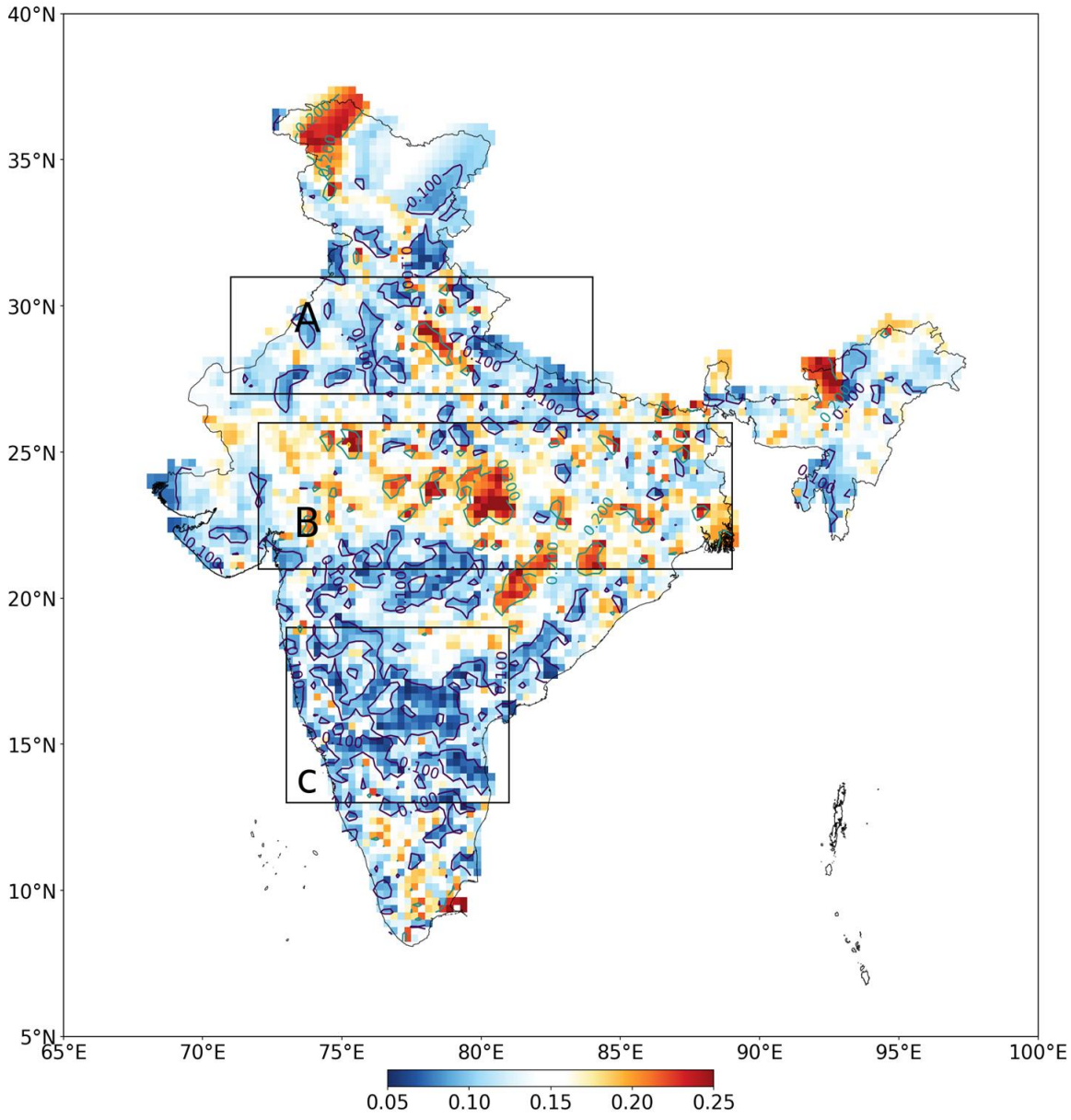

Figure 8. The variability (standard deviation) in the correlation between ISMR and running correlation Niño3.4 time series

The plot shows the spatial map of running correlation with standard deviation. A 30-year running correlation is carried out between rainfall at each grid points in the Indian region and Nino 3.4 SST (JJAS monthly anomaly) from 1901-2018 to distinctly point out the regions of variability. The standard deviation of the running correlation denotes the variability in correlation over time. Regions were identified where the correlation is most

variable or comparatively less variable in time and three boxes were selected. The three boxes A (71˚E, 84 ˚E, 27 ˚ N, 31 ˚N), B (72 ˚E, 89 ˚E, 21 ˚N, 26 ˚N), C (73 ˚E, 81 ˚E, 13 ˚N, 19 ˚N) corresponding to north, central and south India represent moderate, largely variable and low correlation respectively with the Niño3.4 time series. We observe low variation in correlation at the southern peninsula. The moderate variation in correlation was observed in the North Indian region. The greatest variation is observed at the Central Indian region box.

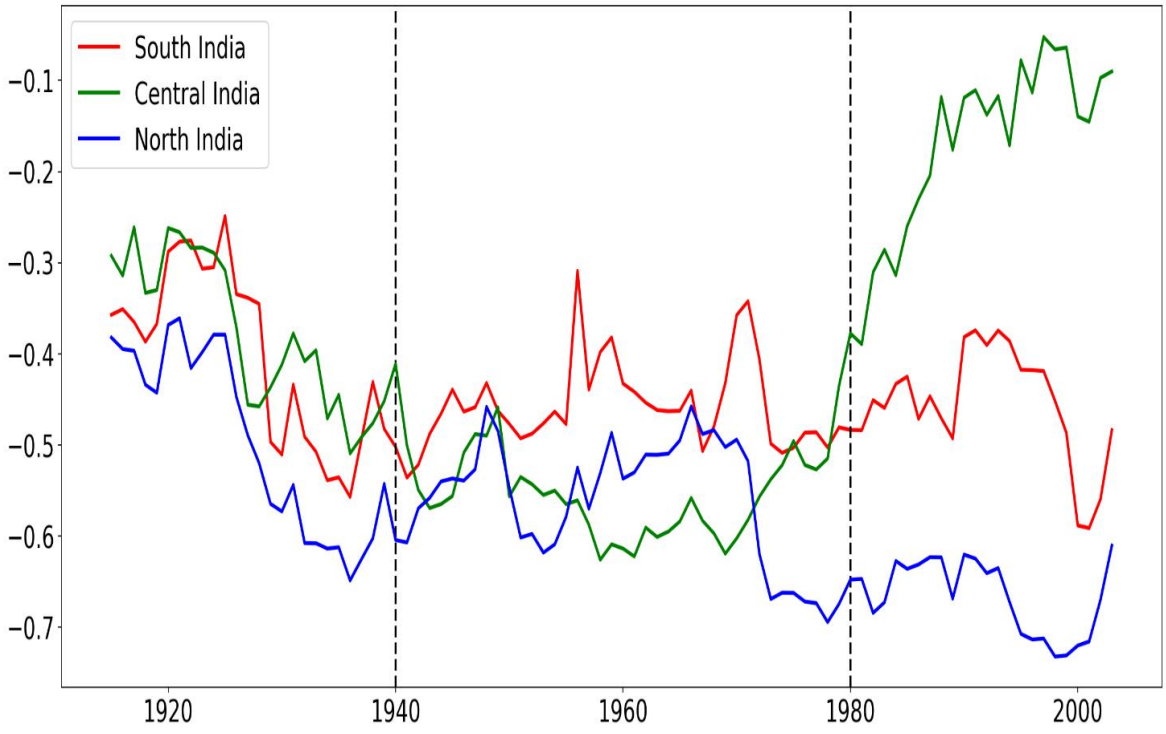

Figure 9. shows the 30-year running correlation between the mean rainfall at the three boxes (north, central and south) and Niño3.4 SST

South India shows a more consistent relationship with the Niño3.4 time series over the last century. Therefore, the running correlation has not varied much over this region (the correlation value varies between -0.3 to -0.6). The

correlation between north India and Niño3.4 time series is observed to be increased (from - 0.4 to -0.7). Central India shows the most variable relation with Nino 3.4 SST. From 1901 to 1940 the correlation between rainfall at central India and Niño3.4 was weak (approximately -0.3 to -0.5). During the period 1940 to 1980, strong correlation was observed (approximately -0.5 to -0.6). Again, during the recent period (1980 to present), the correlation with Niño3.4 has become weak (approximately between -0.1 to -0.3).

It can be seen that the correlation changes significantly for north, central and south India after 1980. Before 1980 the correlation varied similarly at all 3 boxes. For north India the correlation becomes more negative after 1980 and it becomes stronger. Central India shows very less correlation in the recent years. South India shows a stable negative correlation ranging between -0.3 to -0.6 for the entire period. This figure is a representation of how the ENSO-monsoon relationship has varied for three different regions at different periods of time.

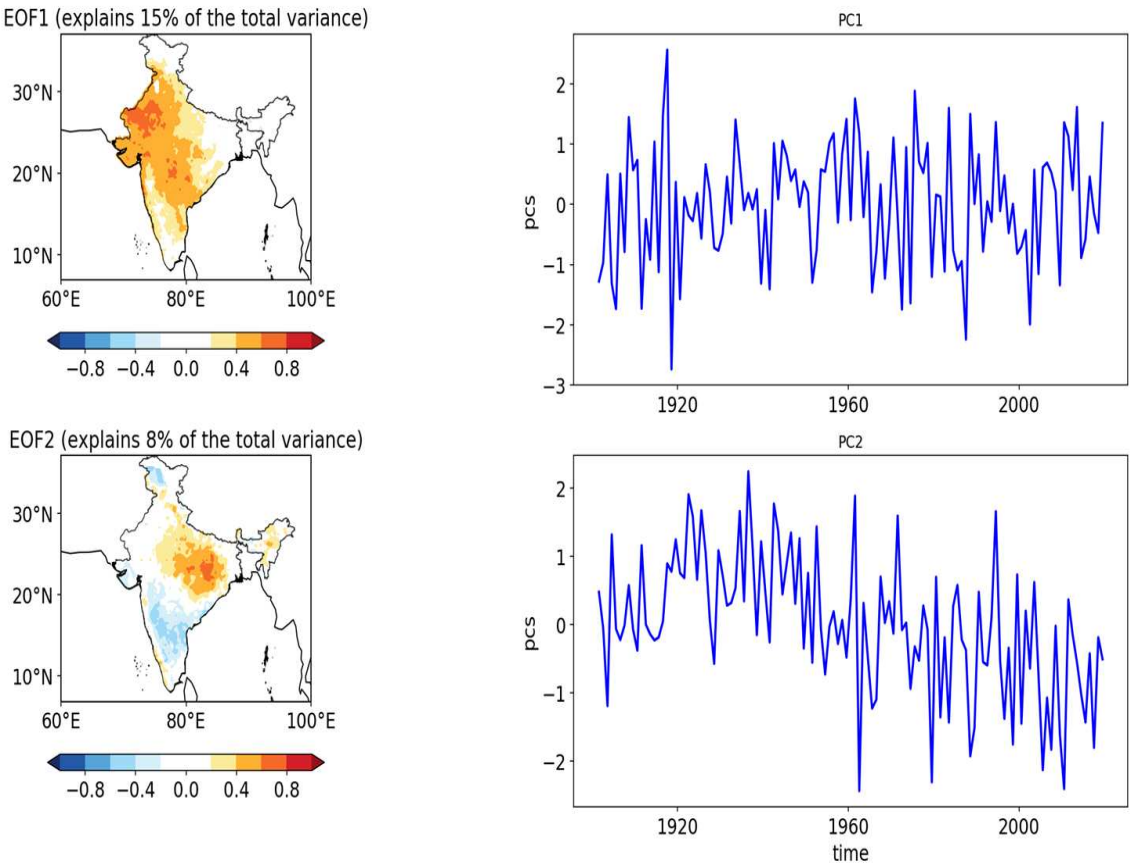

Figure 10. EOF of rainfall normalised at each grid point

Figure 3 shows the EOF of ISMR from 1901 to 2018. To isolate the dominant mode of spatial variability pattern and to find the major drivers of ISMR variability EOF analysis was carried out. The 1st mode shows positive rainfall anomalies over India mainly in the central and western parts. The 1st mode explains 16% of the total variance. The timeseries corresponding to the first mode is named as principle component 1 (PC1). A dipole pattern is seen in the 2nd mode of EOF in which positive rainfall anomalies are present in Gangetic plains and negative anomalies are seen in south India. Positive correlation is seen in east India whereas negative correlation is observed over south India. EOF2 explains 7% of the total variance. PC2 which indicates the second mode of EOF shows a decreasing trend. This means that the positive

and negative rainfall anomaly pattern over Gangetic plains and southern peninsula is reducing respectively. Similar EOF analysis to identify ISMR drivers were also identified by Mishra *et al.,* (2012).

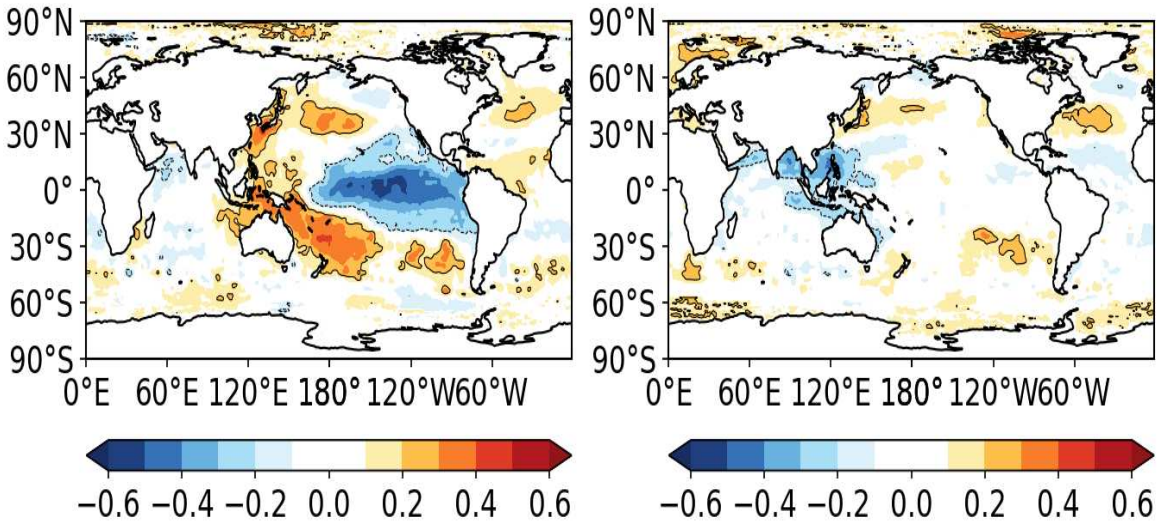

Figure 11. Correlation of global SST with a) PC1 and b) PC2

The global SST anomaly is correlated with principle component 1 and 2. PC1 shows a negative correlation with SST over Nino 3.4 region. This means that the positive rainfall anomalies over India in the EOF 1 mode is associated with the negative SST anomalies over the Nino 3.4 region. Hence, we can confirm ENSO as the cause for the first mode of variability. When global SST was correlated with PC2, a negative correlation can be seen over Arabian sea, Bay of Bengal and South China sea. So, the positive rainfall anomalies over the Gangetic plains and negative anomalies over the southern peninsula is related to the negative SST anomalies over Arabian sea, Bay of Bengal and South China sea.

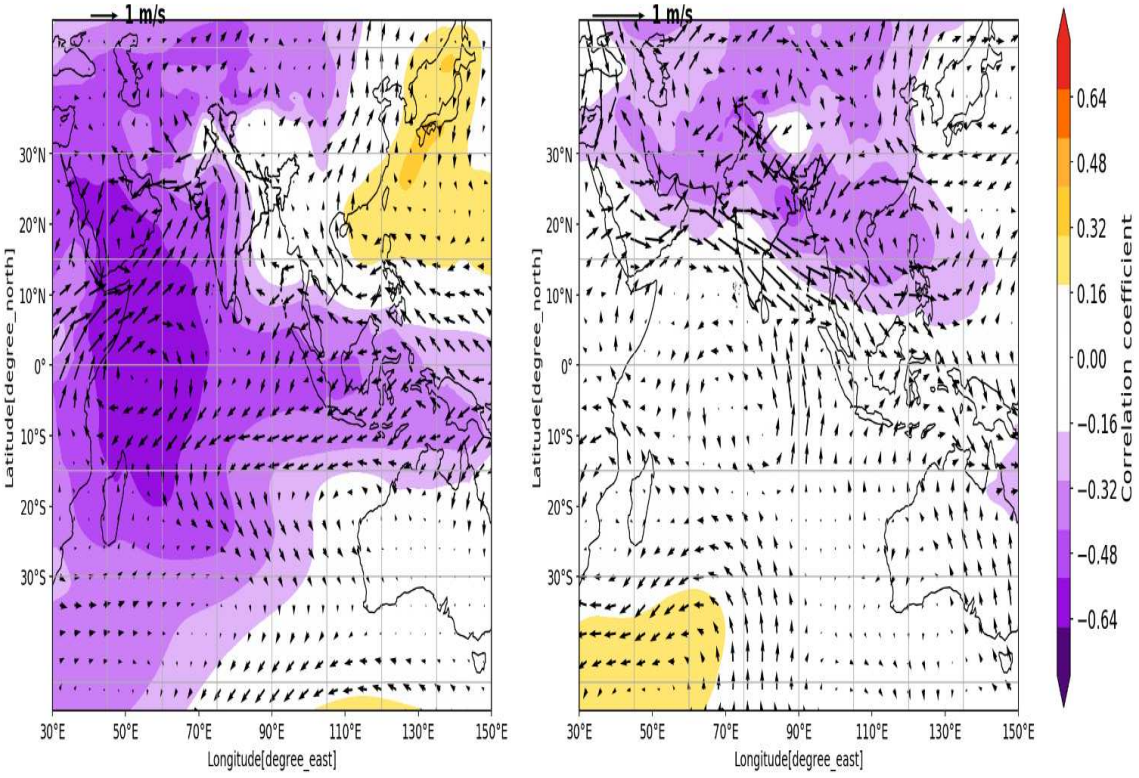

Figure 12. Correlation of a) PC1 and b) PC2 with wind and geopotential height

The figure 5a. gives the correlation between PC1 with wind at 700 hPa and 850 hPa geopotential height. South westerly winds are prevalent over India conducive for heavy rainfall. Also, negative geopotential values indicating a low-pressure region are seen over the Indian subcontinent. These indicate that higher rainfall anomalies are present in India in the PC1 mode which underscores the previous analysis. In figure 5b. westerly winds are present which carry moisture from the Arabian sea to the Bay of Bengal favourable for the formation of depressions. Negative geopotential values are seen over the monsoon trough region indicating greater rainfall. The strength of the monsoon trough is dependent on the frequency of depressions over Bay of Bengal. So, it can be said that EOF2, the second major driver corresponds to monsoon trough/ depressions.

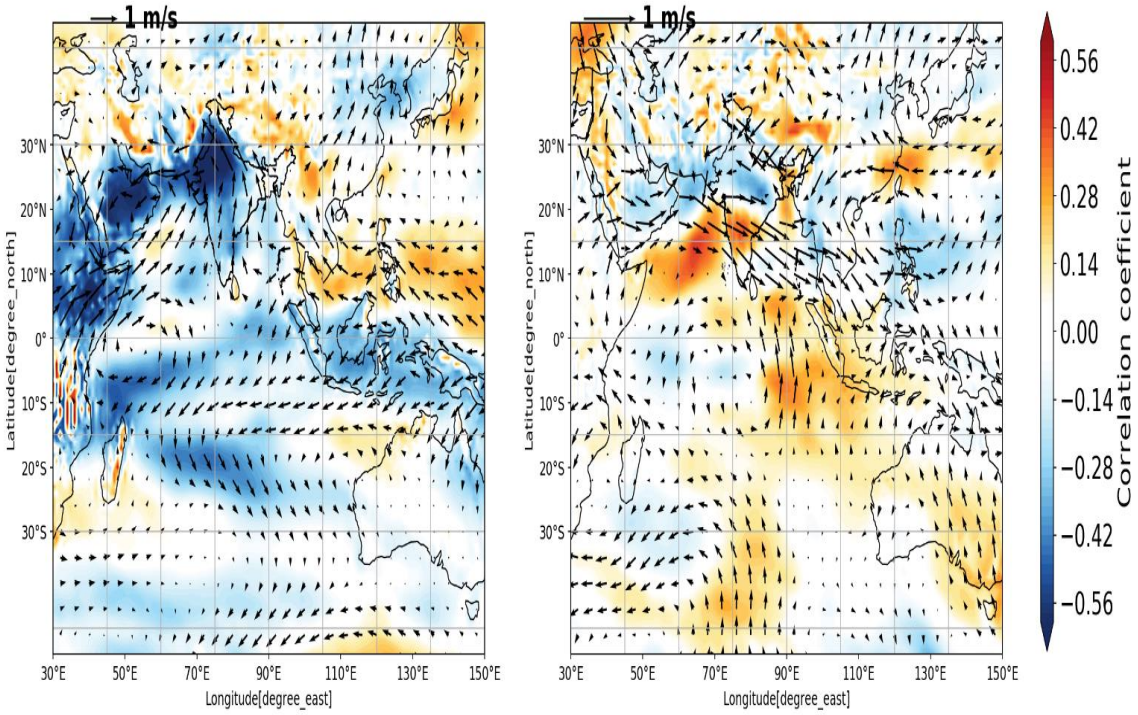

Figure 13. Correlation of a) PC1 and b) PC2 with omega and geopotential height

Figure 6a. shows the correlation of PC1 with wind at 700 hPa and omega at 500 hPa. Negative omega values which indicate ascending motion can be noticed over India. Figure 6b. represents correlation of PC2 with wind at 700 hPa and omega at 500 hPa. Low omega values can be seen over the monsoon trough region and high values over south India which corresponds to high and low rainfall anomalies respectively.

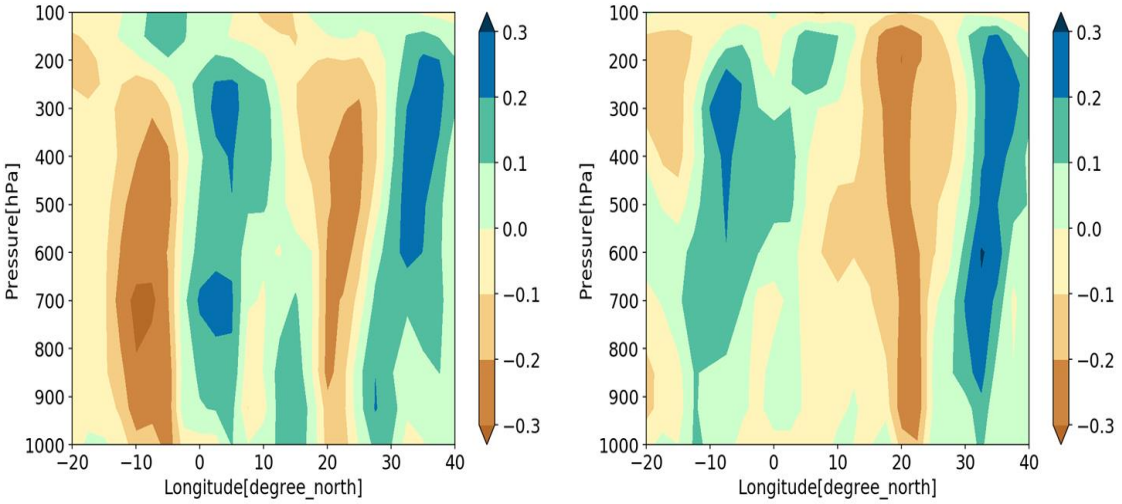

Figure 14. correlation of vertical velocity for the zonal mean of the entire longitude from 1901 to 2018 during JJAS with a) PC1 and b) PC2 respectively

Figure 14. shows the correlation of vertical velocity for the zonal mean of latitude 20°S to 40°N for the period 1901 to 2018 during JJAS with a) PC1 and b) PC2 respectively. Figure 14a. shows subsidence at equatorial region with positive omega values. Figure 14b. shows convergence over the monsoon trough region (20 ˚ N to 25 ˚ N) with negative omega values.

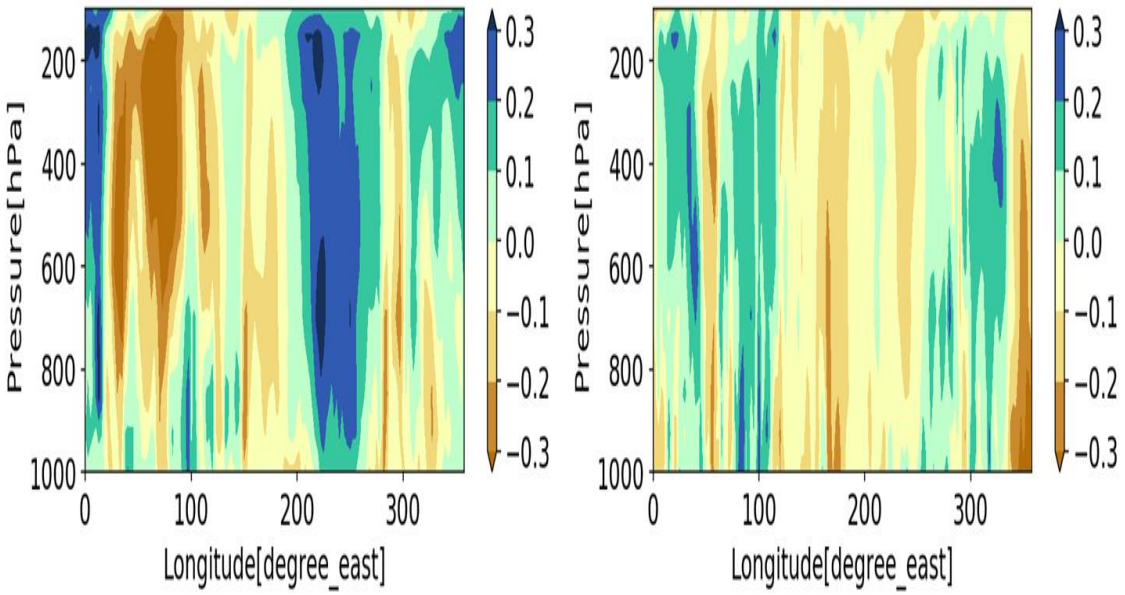

Figure 15. correlation of vertical velocity for the meridional mean of the entire longitude from 1901 to 2018 during JJAS with a) PC1 and b) PC2 respectively

For Figure 15a. there is positive correlation at 240 to 300-degree longitude which indicates subsidence and on the western Pacific there is upward motion with negative omega values. Figure 15b. shows positive omega values over eastern Indian Ocean indicating subsidence.

.

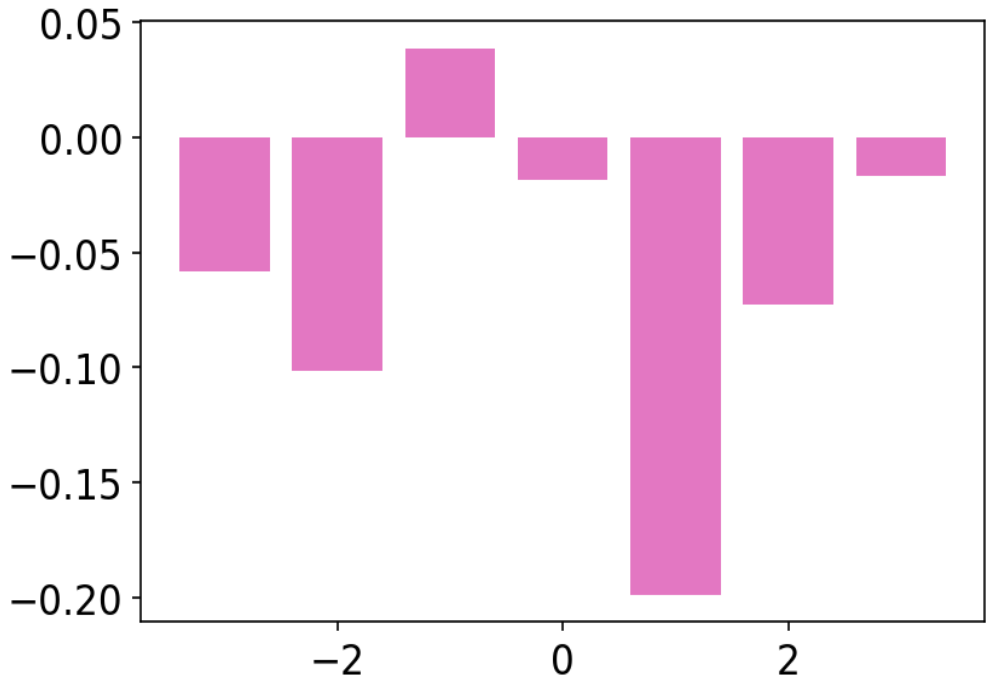

Figure 16. Lead lag correlation between PC2 and Nino 3.4 SST (PC2 lags Nino 3.4 SST)

The figure represents the lead lag correlation between PC2 and Nino 3.4 SST. Here X axis denotes the lag/lead in years and Y axis denotes the correlation coefficient. There is maximum correlation at 1 which indicates that the PC2 lags Nino 3.4 SST by 1 year. The rainfall anomalies over the Gangetic plains and south India shows a lagged response to ENSO. At the time of El Niño there is increased net solar radiation and reduced air sea fluxes as well as latent and sensible heat which induce warming of the Indian Ocean and the positive SST anomalies can sustain till the following JJAS (Mishra *et al.,* 2012).

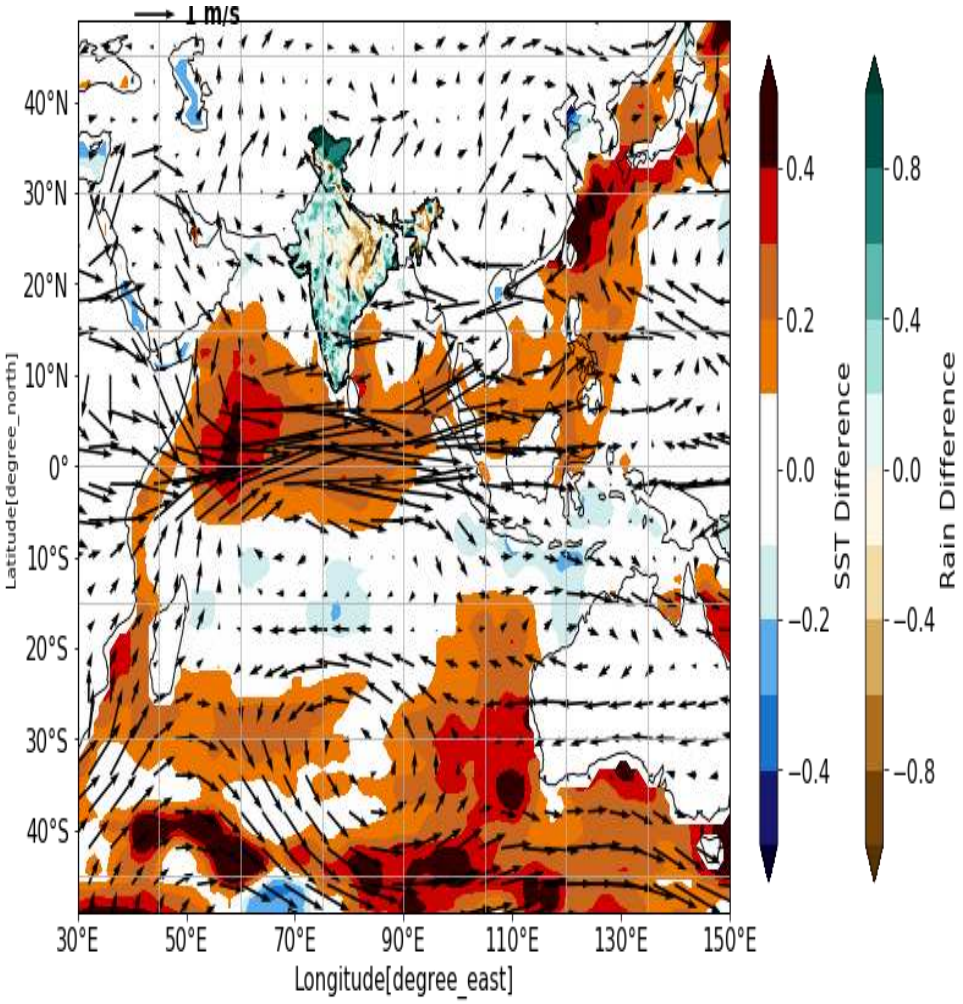

Figure 17. Trend in ISMR and SST (JJAS)

The figure shows the trend in relative SST (difference between global SST and tropical mean SST), ISMR and the circulation pattern which is the difference in wind (recent – earlier) between 1901 to 1957 and 1958 to 2015. Positive SST anomalies in the western Indian Ocean denotes enhanced warming which reduces the south westerly winds and the prominence of anomalous easterly winds which reduce mid tropospheric moisture transport from Arabian Sea. This leads to a reduction in the number of monsoon depressions and consequently the weakening of monsoon trough which can be observed from the negative rainfall anomalies over the monsoon trough region. This is consistent with the analysis carried out by Vishnu *et al.,* (2016)

who found a decreasing trend in the number of monsoon depressions over Bay of Bengal due to the lessening of mid tropospheric humidity.

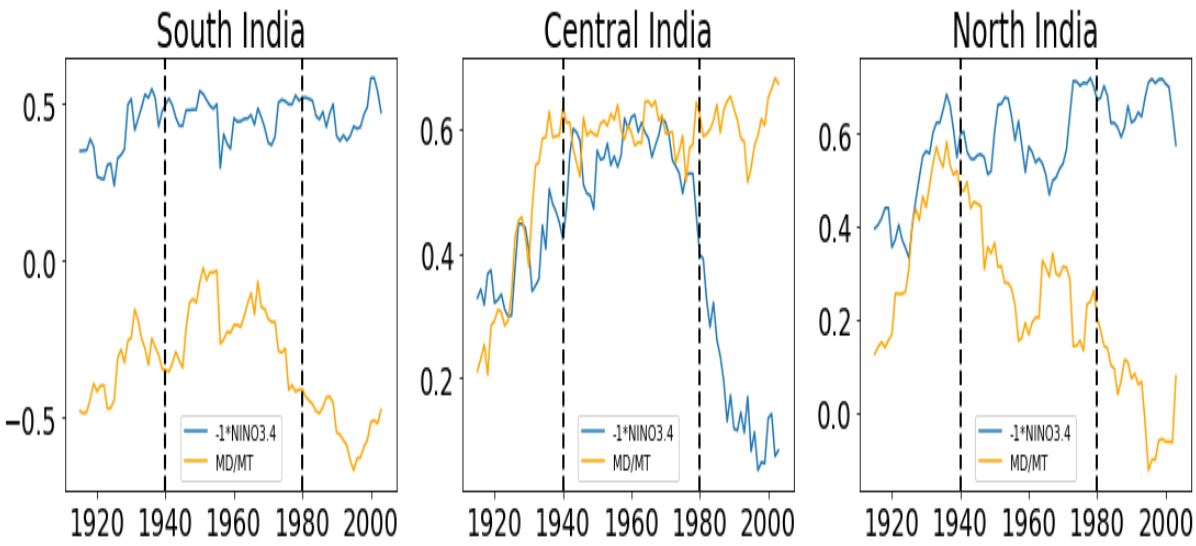

Figure 18. 30 year running correlation of a) south India rainfall with Nino 3.4 SST and Monsoon trough/depressions b) central India rainfall with Nino 3.4 SST and Monsoon trough/depressions c) north India rainfall with Nino 3.4 SST and Monsoon trough/depressions

The figure shows the 30-year running correlation carried out for each box with the two major drivers identified: negative Nino 3.4 SST (which denotes variability due to ENSO) and monsoon trough/depressions. In the first case, for south India (figure 11a) the influence of both the factors are dominant which means that south India rainfall is dependent on ENSO variability as well as monsoon trough/depressions. In figure 11b. for central India, the contribution by ENSO and monsoon trough/depressions are increasing up to 1980 and then the contribution by ENSO started declining drastically. But the influence of monsoon trough and depressions remained powerful. For north India (figure 11c) the influence of ENSO is increasing and has become stronger in the recent period while the impact of monsoon trough/depression is decreasing.

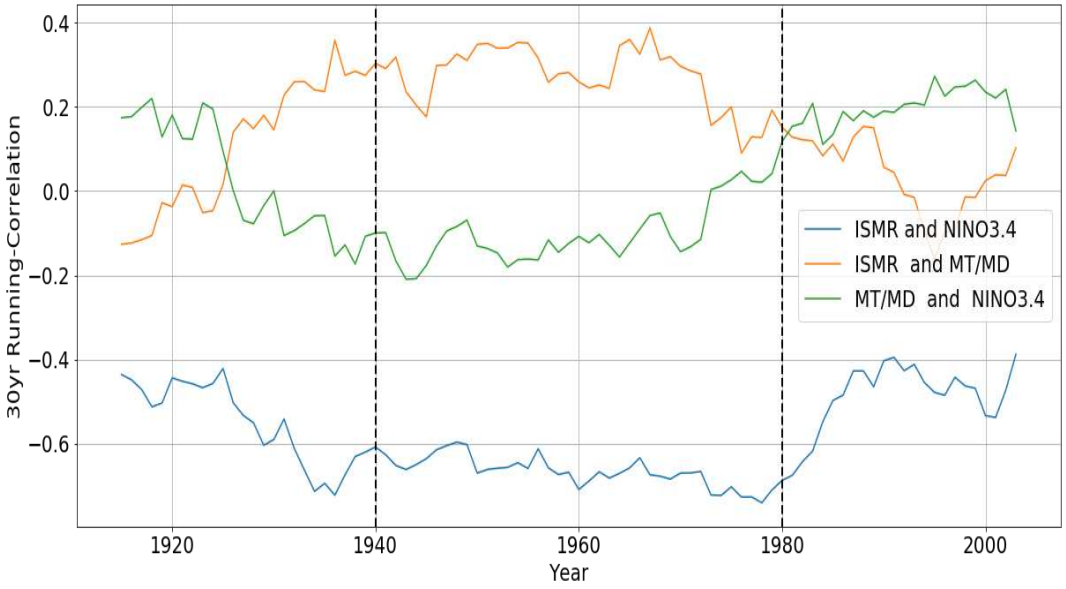

Figure 19. Running correlation of ISMR with Nino 3.4 and monsoon trough/depressions and monsoon trough/depression with Nino 3.4

From the figure it can be seen that in the middle period from 1940 to 1980 the correlation of ISMR with Nino 3.4 as well as monsoon trough/depression has increased. It is also worthy to note that ISMR and monsoon trough/depression exhibits slightly negative correlation from 1940 to 2018. This means that the two major drivers are not fully independent but there is some connection between the two.

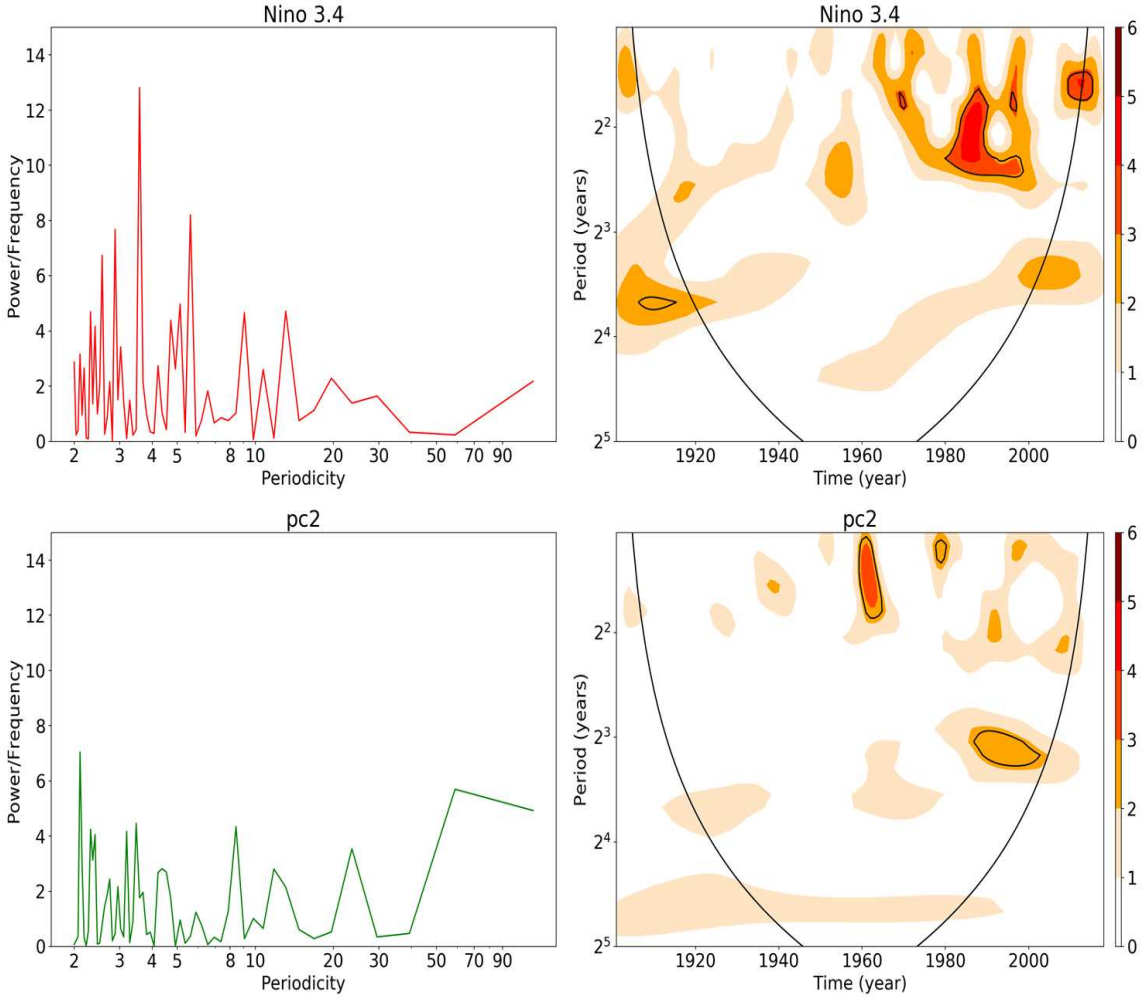

Figure 20. Power spectrum and wavelet analysis of Nino 3.4 SST and PC2

The periodicity present in the timeseries and the corresponding timescale can be identified from the power spectrum and wavelet analysis respectively. The 2-7 years periodicity associated with ENSO can be seen in the power spectrum of Nino 3.4 SST. A decadal variability is also visible for it. The wavelet analysis of Nino 3.4 SST shows that 2-8-year periodicity is more prominent after 1960. For PC2 the power spectrum shows both 2-7 years periodicity and a decadal variability which is more prominent here. In the wavelet analysis it can be seen that 2-4 years variability is seen in the year 1960 and a decadal variability is seen after 1980.

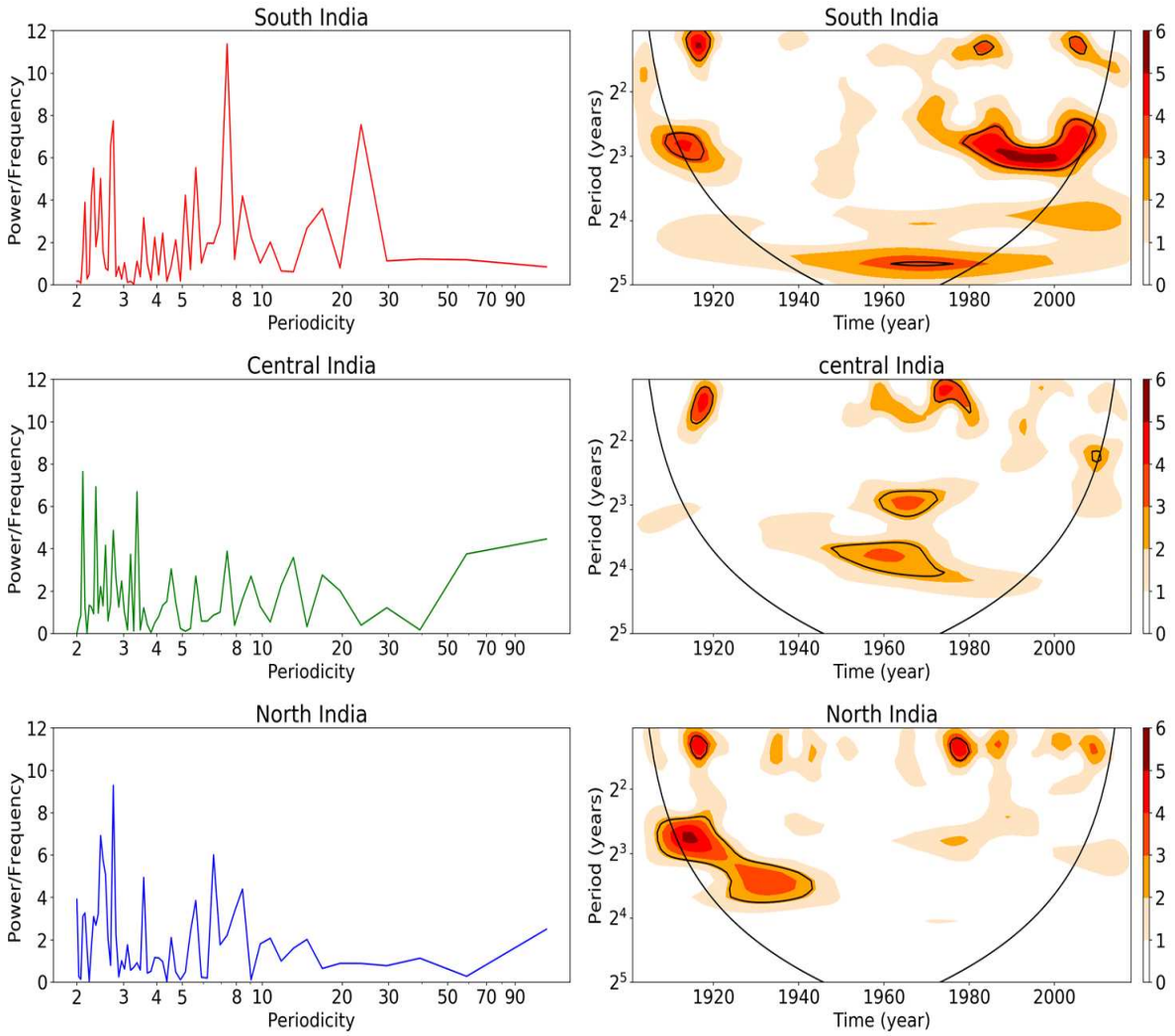

Figure 21. Power spectrum and wavelet analysis for north, central and south India

In order to identify the frequency present in each of the timeseries of north, central and south India box the power spectrum is drawn and to identify the time scale in which these frequencies are present, wavelet analysis is carried out. For South India 2 to 8 years periodicity signals are prominent in years up to 1920 and then from 1980 to 2000 which is similar to that of Nino 3.4 SST. A decadal variability is also seen for south India which means that there is a connection with PC2 also. Central India shows frequency signal between 2 to 4 years during 1910 to 1920 and 1960 to 1980. The power spectrum of central India resembles that of PC2. For north India up to 8 years

of periodicity signal peaks can be seen during the years 1910 to 1930. Comparing it with the power spectrum and wavelet analysis of Nino 3.4 and PC2 it is seen that north India rainfall is dependent on Nino 3.4 SST and not on PC2 because it does not exhibit decadal variability. The frequency of events is quite stable and high for south India. For central India the frequency is comparatively lower than that of north India. It is clear from this analysis that South India shows relation with both ENSO and monsoon trough/depressions, central India exhibits relation with only monsoon trough/depressions and north India has its relation with ENSO only.

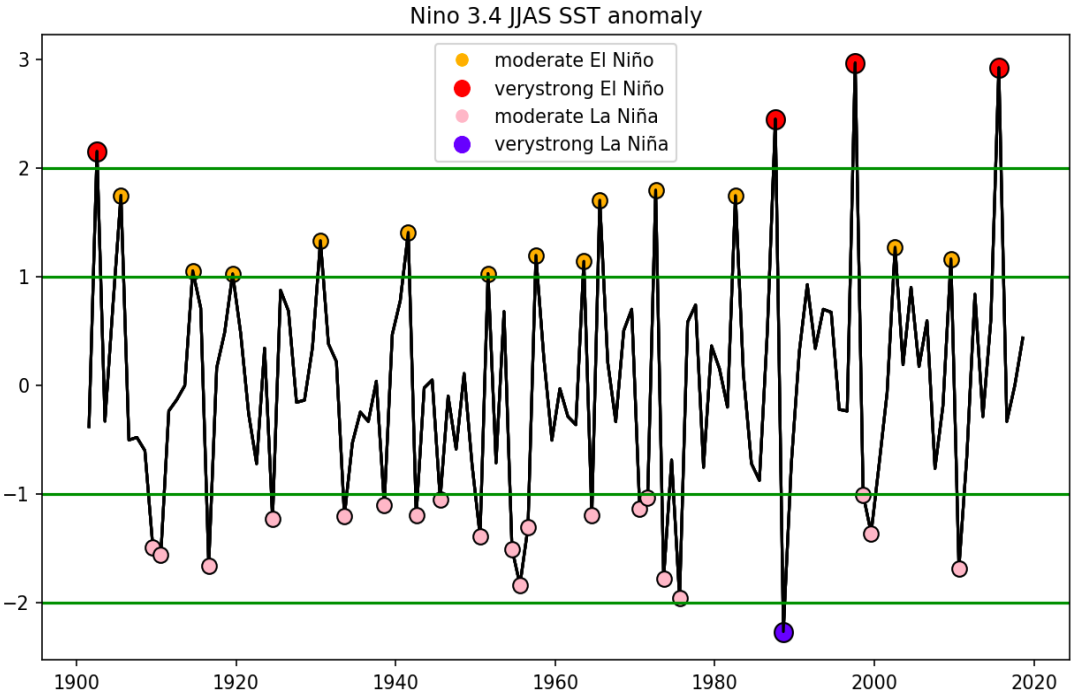

Figure 22. Nino 3.4 SST anomaly during JJAS for the period 1901 to 2018

The Nino 3.4 SST anomaly is standardized and plotted as timeseries. Moderate El Niño years are selected which cross 1 standard deviation and which is less than 2 standard deviation (1905, 1914, 1919, 1930, 1941, 1951, 1957, 1963, 1965, 1972, 1982, 2002, 2009). The anomaly values which cross 2 standard deviation correspond to very strong El Niño years (1902, 1987, 1997, 2015). Similarly moderate La Niña years are chosen which is greater than -1 and less than 2 standard deviation (1909, 1910, 1916, 1924, 1933, 1938, 1942, 1945, 1950, 1954, 1955, 1956, 1964, 1970, 1971, 1973, 1975, 1998, 1999, 2010). Very strong La Niña years are selected which cross -2 standard deviation (1988). It can be seen that the frequency of very strong El Nino and La Nina events is comparatively more after 1980 than in the early years. Hence it is important to study the effects caused by very strong ENSO on the monsoon rainfall of India.

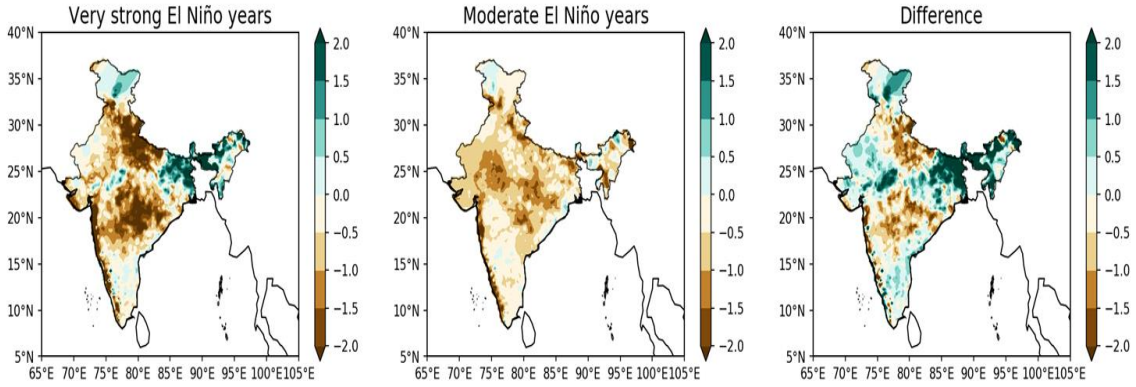

Figure 23. Composite of rainfall anomaly during very strong El Niño, moderate El Niño and the difference between the two

The figure 23 shows the composite of rainfall anomaly during very strong El Niño, moderate El Niño and their difference, which is calculated to see what are the additional changes that took place in a very strong El Niño. At the time of very strong El Niño, the regions with negative rainfall anomalies are south, central India, north India and Western Ghats region. Central India and north east India experienced positive rainfall anomalies. Moderate El Niño showed negative rainfall anomalies for almost all parts of India. While moderate El Nino led to a reduction of rainfall for almost the entire Indian subcontinent, very strong El Nino had its impacts especially on parts of south-central India. Higher than normal rainfall is present in central India at the time of very strong El Nino.

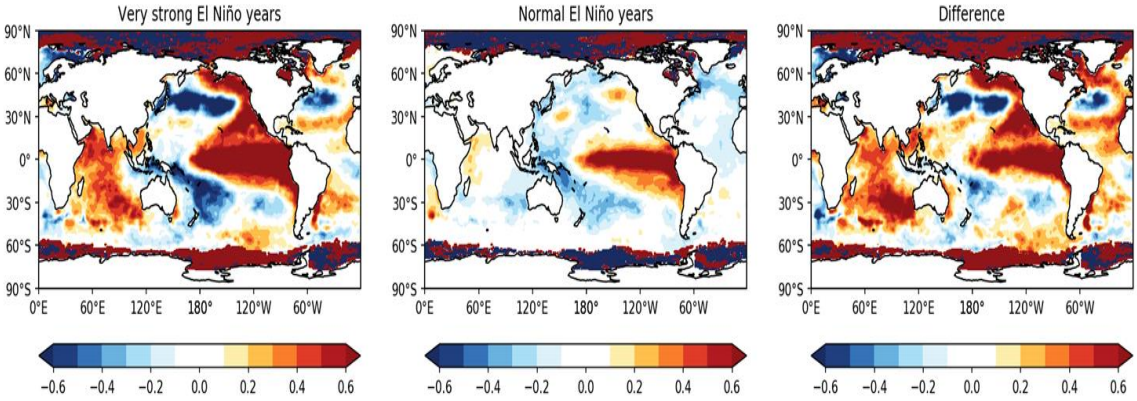

Figure 24. Composite of SST during very strong El Niño, normal El Niño and their difference

The figure 24 shows the composite of global SST during very strong El Niño, moderate El Niño and their difference. Positive SST anomalies are seen in eastern Pacific and Indian Ocean during very strong El Nino. During moderate El Niño positive SST anomalies are present only in eastern Pacific. At the time of very strong El Nino, there is warming of both eastern pacific and Indian Ocean but there is warming of only eastern Pacific during moderate El Nino years.

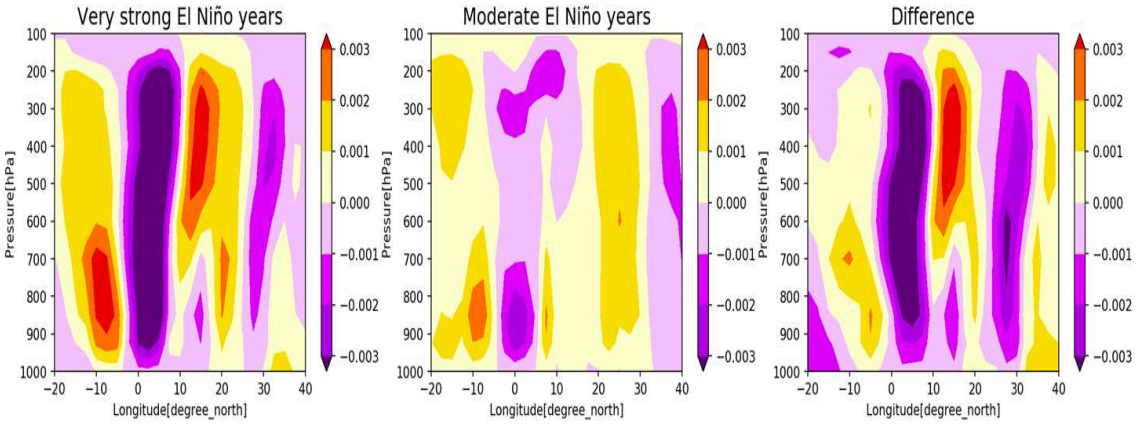

Figure 25. Hadley circulation during very strong El Niño, moderate El Niño and their difference

The figure 25. shows Hadley circulation during very strong El Nino, moderate El Nino events and the difference between them. During very strong El Niño years there is anomalous subsidence over the Indian subcontinent with positive omega values and hence a reduction in the rainfall. Moderate El Niño years show anomalous subsidence over north India.

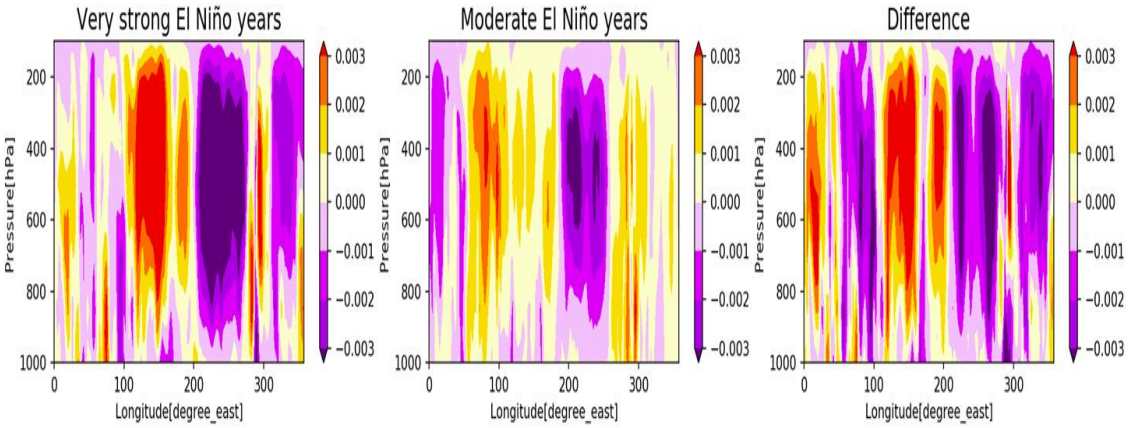

Figure 26. Walker circulation during very strong El Niño normal El Niño and their difference

The figure 26. represents Walker circulation during very strong El Nino, normal El Nino and their difference. During very strong El Niño years, there is negative omega values over eastern Pacific indicating upward motion and positive omega values over western Pacific which shows subsidence.

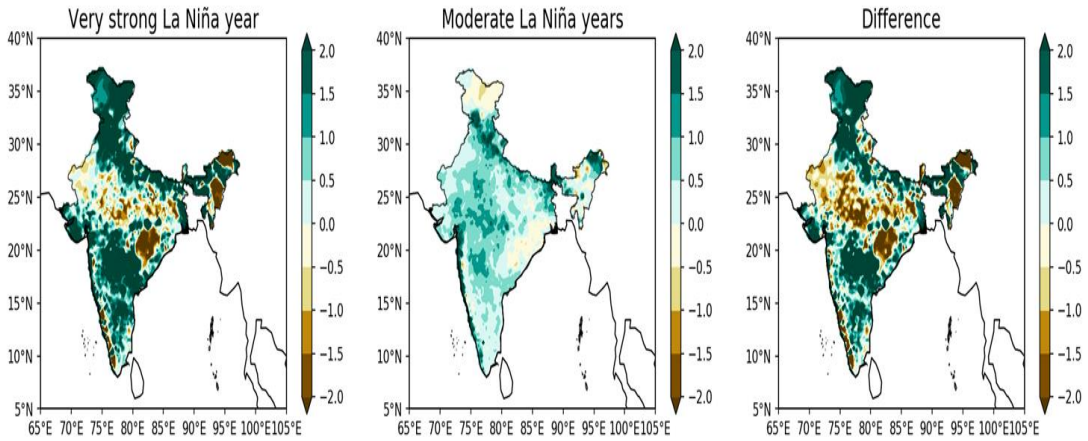

Figure 27. Composite of rainfall anomalies during very strong La Niña year, moderate La Niña years and their difference

The figure 27. shows the composite of rainfall anomalies during very strong La Niña year, moderate La Niña years and their difference. At the time of very strong La Niña year, positive rainfall anomalies are present in north and south India while negative rainfall anomalies are seen in central and east India. During moderate La Niña years positive rainfall anomalies are present over most parts of India. Though very strong La Nina brought intense rainfall to north and south India, central India experienced low rainfall pattern.

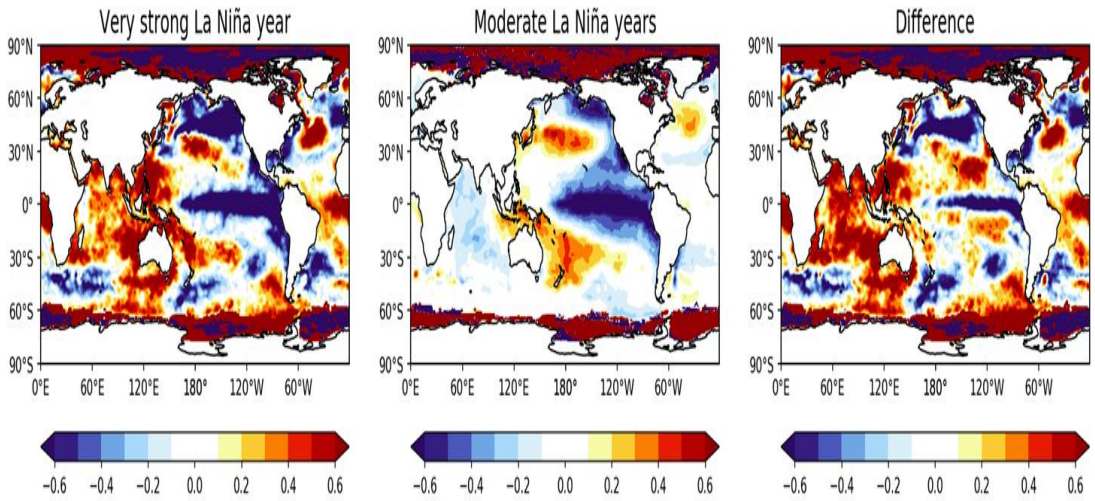

Figure 28. Composite of SST anomalies during very strong La Niña year, moderate La Niña years and their difference

The figure 28. represents the composite of SST anomalies during very strong La Niña year, moderate La Niña years and their difference. Very strong La Niña year show negative SST anomalies over eastern Pacific and positive SST anomalies can be seen over Indian Ocean. But during moderate La Niña years negative SST anomalies are seen in eastern Pacific as well as in the Indian Ocean. There is anomalous warming of Indian ocean at the time of very strong La Nina which is comparatively higher than that of very strong El Nino.

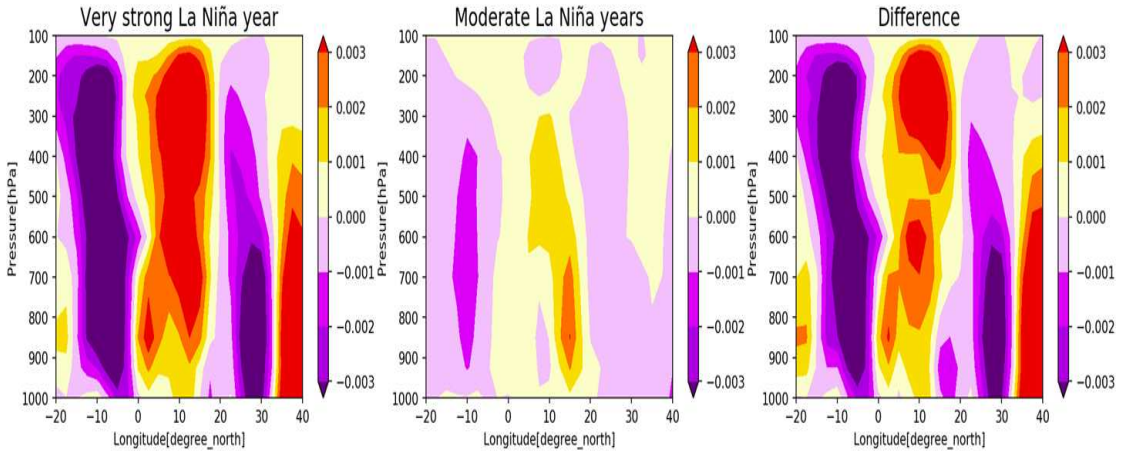

Figure 29. Hadley circulation during very strong La Niña, moderate La Niña and their difference

The figure 29. shows Hadley circulation during very strong La Niña, moderate La Niña and their difference. Very strong La Niña years show anomalous subsidence over the equatorial region and over the Indian subcontinent there is negative omega values which show upward motion there. Moderate La Niña years show convergence over India.

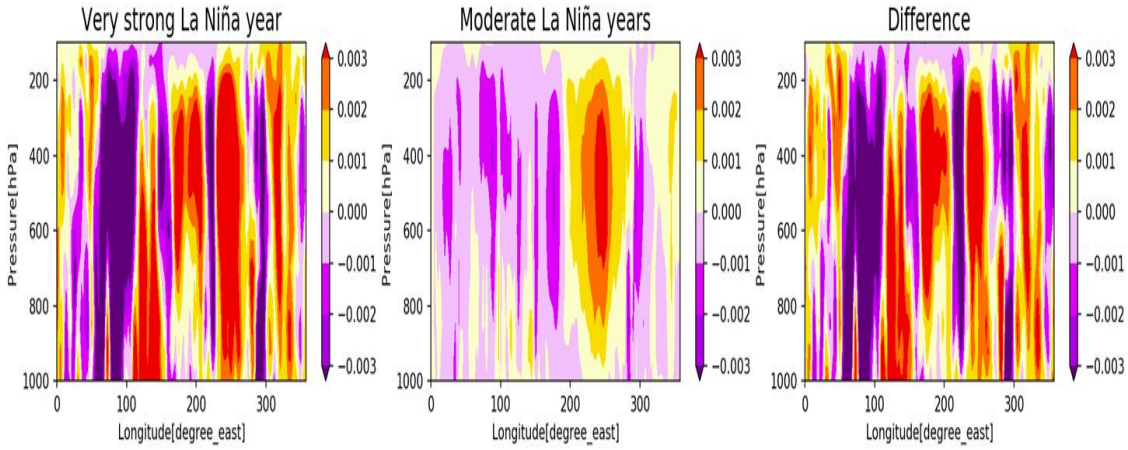

Figure 30. Walker circulation during very strong La Niña, moderate La Niña and their difference

The figure 30. represents Walker circulation during very strong La Niña, moderate La Niña and their difference. During very strong La Niña year positive omega values are seen in the eastern Pacific which indicates anomalous subsidence and over western Indian Ocean there is upward motion. Moderate La Niña years also show subsidence over eastern Pacific.

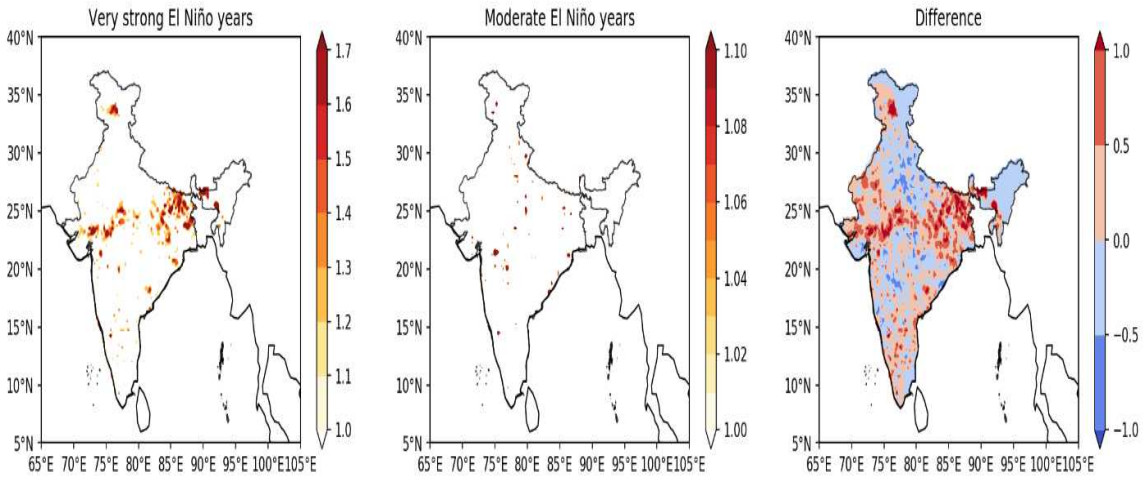

Figure 31. Extreme rainfall events computed using 99.5 percentile threshold criteria for very strong, moderate El Niño years and their difference

The figure shows extreme rainfall events during very strong, moderate El Niño years and their difference. The extreme precipitation events are based on 99.5 percentile threshold value (Nikumbh *et al*., 2019). The number of extreme rainfall events are greater during very strong El Niño years and are mostly confined to central and eastern parts of India. Moderate El Niño years show extreme precipitation events which are scattered.

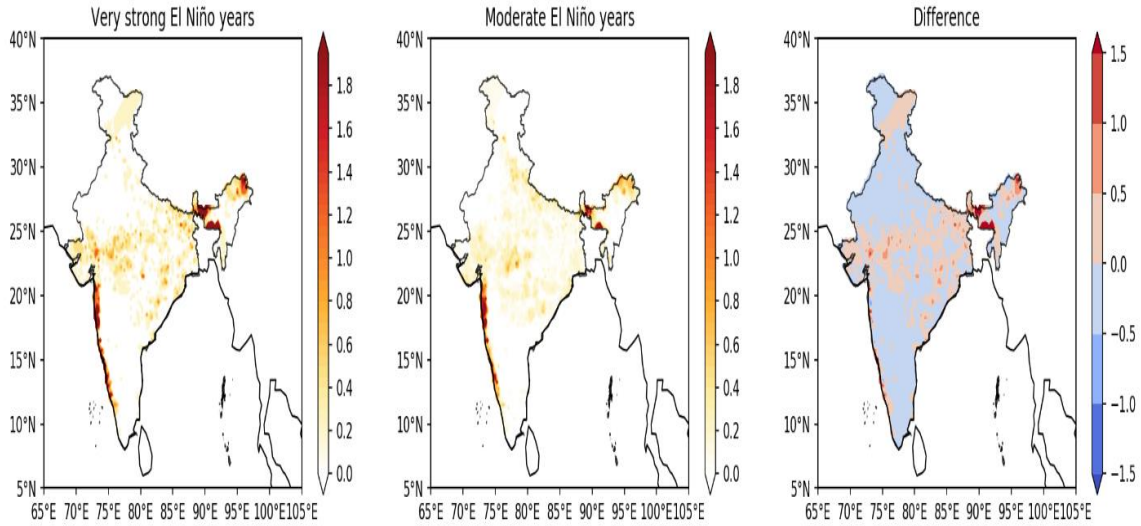

Figure 32. Extreme rainfall events during very strong, moderate El Niño, and their difference based on 150mm/day threshold criteria

The figure shows extreme rainfall events during very strong, moderate El Niño, and their difference. The extreme rainfall events are also categorized based on the events in which the rainfall is greater than 150mm/day (Roxy *et al*., 2017). Very strong El Niño years show extreme precipitation events in central, east India as well as Western Ghats region.

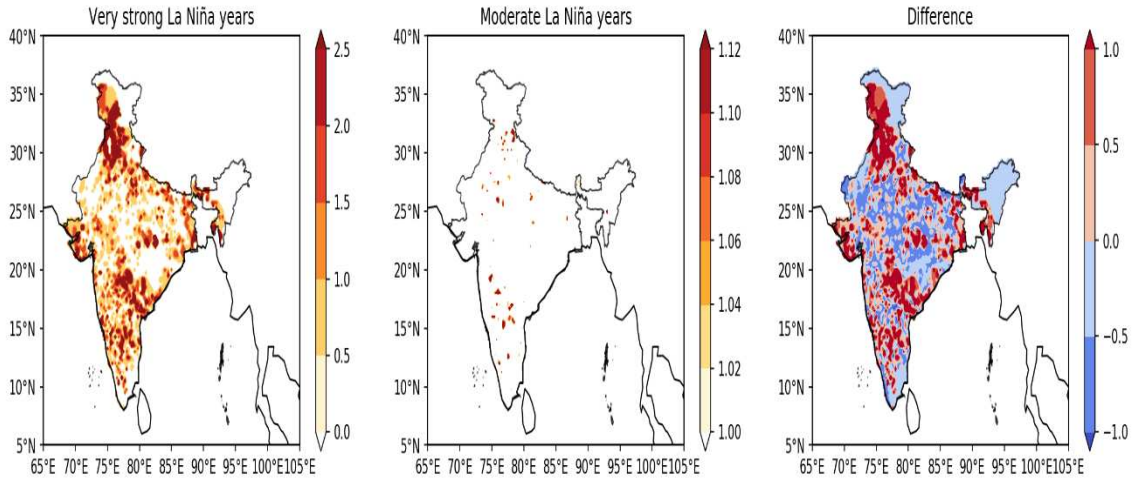

Figure 33. Extreme rainfall events computed using 99.5 percentile threshold criteria during very strong La Niña year, moderate La Niña years and their difference

The figure shows extreme rainfall events during very strong La Niña year, moderate La Niña years and their difference. The extreme precipitation events based on 99.5 percentile threshold (Nikumbh *et al*., 2019) is calculated during very strong and moderate La Niña years. The extreme rainfall events are present mostly in southern and northern parts of India during very strong La Niña year.

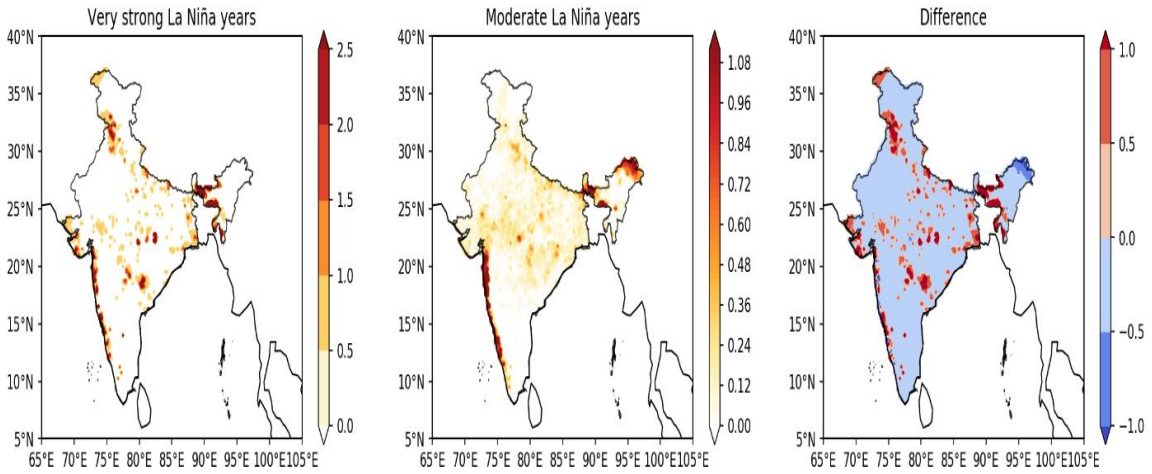

Figure 34. Extreme rainfall events computed using 150mm/day threshold criteria during very strong La Niña year, moderate La Niña years and their difference

The figure shows extreme rainfall events computed using 150mm/day threshold criteria during very strong La Niña year, moderate La Niña years and their difference. Extreme rainfall events are calculated based on 150mm/day threshold (Roxy *et al*., 2017). During very strong La Niña extreme precipitation events are seen in Western Ghats region, and parts of south India.

CHAPTER 5

SUMMARY AND CONCLUSION

El Niño Southern Oscillation is a coupled ocean-atmospheric phenomenon that takes place in the tropical Pacific Ocean. ENSO has two phases: the warm phase corresponds to El Niño and the cold phase is the La Niña. This climatic oscillation between a warm period and cold period is referred to as Southern Oscillation. During El Niño warm SST anomalies are prevalent over the east equatorial Pacific and cold SST anomalies over the west equatorial Pacific. El Niño brings about good amount of rainfall over the east equatorial Pacific region (Peru coast) whereas reduced rainfall prevails over the western part of the equatorial Pacific (Australia, the Indian subcontinent). The reverse happens for La Niña. The walker circulation reverses during these warm and cold phases.

ENSO related vagaries of Indian monsoon exhibit diversity in both time and space. With its varying influence on different regions of the country at different points of time, the implications posed by ENSO is quite dramatical. El Niño, has an out of phase relationship with the Indian summer monsoon, with a drastic reduction in the amount of rainfall. However, this does not hold true for the entire period monitored from 1901 to 2018. For the purpose of investigating the changing relationship, the 118-year study period was divided into early (1901 to 1940), middle (1941 to 1980) and the recent epochs (1981 to 2018). This division of years and the subsequent analysis revealed that the ENSO-monsoon inverse relationship started rising from the point of initiation, became stable and declined in the recent epoch. Also, it is of interest to note that South India does not exhibit considerable variation in the relationship whereas North India shows increasing relationship. On the contrary, central India rainfall association with ENSO diminishes in the recent decade.

The key drivers of Indian summer monsoon variability were detected in order to point out the culprit that has caused this altered interrelationship.

This has led to the identification of monsoon trough and depressions as another cause in addition to ENSO phenomenon though the contribution of the former is not as distinguished as the latter. From the subsequent analysis it became evident that the role of monsoon trough and depressions emerged as the primary cause of rainfall variability over central India that surpassed the role of ENSO related variability. For south India rainfall, ENSO related variability and the influence of monsoon trough and depressions work hand in hand. North India rainfall has an increasing relation with ENSO while the role of monsoon trough and depression is declining. Since the association of Indian monsoon with ENSO is inarguably impactful on the Indian subcontinent, the consideration of extreme ENSO events and its repercussions on the rainfall pattern is no less important. Central India showed greater rainfall at the time of very strong El Niño and extreme precipitation events were also notably present during this time. Increased rainfall pattern was observed in north and south India at the time of very strong La Niña years except parts of central India where the rainfall was considerably less. Hence, we can conclude that ENSO plays a dynamic role during the southwest monsoon season with extreme ENSO years being exceptionally mysterious for the central India

REFERENCES

Abram, N.J., Gagan, M.K., Cole, J.E., Hantoro, W.S. and Mudelsee, M., 2008. Recent intensification of tropical climate variability in the Indian Ocean. Nature Geoscience, 1(12): 849-853.

Aceituno, P., 1992. El Niño, the Southern Oscillation, and ENSO: Confusing names for a complex ocean–atmosphere interaction. Bulletin of the American Meteorological Society, 73(4): 483-485.

Ajayamohan, R.S. and Rao, S.A., 2008. Indian Ocean dipole modulates the number of extreme rainfall events over India in a warming environment. Journal of the Meteorological Society of Japan. Ser. II, 86(1): 245-252.

Allan, R.P. and Soden, B.J., 2008. Atmospheric warming and the amplification of precipitation extremes. Science, 321(5895): 1481-1484.

Anil, N., Kumar, M.R., Sajeev, R. and Saji, P.K., 2016. Role of distinct flavours of IOD events on Indian summer monsoon. Natural Hazards, 82(2): 1317-1326.

Ashok, K. and Saji, N.H., 2007. On the impacts of ENSO and Indian Ocean dipole events on sub-regional Indian summer monsoon rainfall. Natural Hazards, 42(2): 273-285.

Ashok, K., Behera, S.K., Rao, S.A., Weng, H. and Yamagata, T., 2007. El Niño Modoki and its possible teleconnection. Journal of Geophysical Research: Oceans, 112(C11).

Ashok, K., Guan, Z. and Yamagata, T., 2001. Impact of the Indian Ocean dipole on the relationship between the Indian monsoon rainfall and ENSO. Geophysical Research Letters, 28(23): 4499-4502.

Ashok, K., Guan, Z., Saji, N.H. and Yamagata, T., 2004. Individual and combined influences of ENSO and the Indian Ocean dipole on the Indian summer monsoon. Journal of Climate, 17(16): 3141-3155.

Bamzai, A.S. and Shukla, J., 1999. Relation between Eurasian snow cover, snow depth, and the Indian summer monsoon: An observational study. Journal of Climate, 12(10): 3117-3132.

Barber, R.T. and Chavez, F.P., 1983. Biological consequences of El Niño. Science, 222(4629): 1203-1210.

Barde, V., Nageswararao, M.M., Mohanty, U.C., Panda, R.K. and Ramadas, M., 2020. Characteristics of southwest summer monsoon rainfall events over East India. Theoretical and Applied Climatology, pp.1-18.

Brown, B.E., 1990. Damage and recovery of coral reefs affected by El Niño related seawater warming in the Thousand Islands, Indonesia. Coral reefs, 8(4): 163-170.

Cai, W., Borlace, S., Lengaigne, M., Van Rensch, P., Collins, M., Vecchi, G., Timmermann, A., Santoso, A., McPhaden, M.J., Wu, L. and England, M.H., 2014. Increasing frequency of extreme El Niño events due to greenhouse warming. Nature climate change, 4(2):111-116.

Cai, W., Wang, G., Santoso, A., McPhaden, M.J., Wu, L., Jin, F.F., Timmermann, A., Collins, M., Vecchi, G., Lengaigne, M. and England, M.H., 2015. Increased frequency of extreme La Niña events under greenhouse warming. Nature Climate Change, 5(2): 132-137.

Capotondi, A. and Sardeshmukh, P.D., 2015. Optimal precursors of different types of ENSO events. Geophysical Research Letters, 42(22): 9952-9960.

Capotondi, A., Wittenberg, A.T., Newman, M., Di Lorenzo, E., Yu, J.Y., Braconnot, P., Cole, J., Dewitte, B., Giese, B., Guilyardi, E. and Jin,

F.F., 2015. Understanding ENSO diversity. Bulletin of the American Meteorological Society, 96(6): 921-938.

Chakraborty, A. and Agrawal, S., 2017. Role of west Asian surface pressure in summer monsoon onset over central India. Environmental Research Letters, 12(7), p.074002.

Chakraborty, A., Nanjundiah, R.S. and Srinivasan, J., 2002. Role of Asian and African orography in Indian summer monsoon. Geophysical research letters, 29(20): 50-1.

Chang, C.P., Harr, P. and Ju, J., 2001. Possible roles of Atlantic circulations on the weakening Indian monsoon rainfall–ENSO relationship. Journal of Climate, 14(11): 2376-2380.

Chen, W., Dong, B. and Lu, R., 2010. Impact of the Atlantic Ocean on the multidecadal fluctuation of El Niño–Southern Oscillation–South Asian monsoon relationship in a coupled general circulation model. Journal of Geophysical Research: Atmospheres, 115(D17).

Cherchi, A. and Navarra, A., 2013. Influence of ENSO and of the Indian Ocean Dipole on the Indian summer monsoon variability. Climate dynamics, 41(1): 81-103.

Chowdary, J.S., Harsha, H.S., Gnanaseelan, C., Srinivas, G., Parekh, A., Pillai, P. and Naidu, C.V., 2017. Indian summer monsoon rainfall variability in response to differences in the decay phase of El Niño. Climate dynamics, 48(7-8): 2707-2727.

Cobb, K.M., Westphal, N., Sayani, H.R., Watson, J.T., Di Lorenzo, E., Cheng, H., Edwards, R.L. and Charles, C.D., 2013. Highly variable El Niño–Southern Oscillation throughout the Holocene. Science, 339(6115): 67-70.

Dimri, A.P., 2013. Relationship between ENSO phases with Northwest India winter precipitation. International journal of climatology, 33(8): 1917-1923.

Dimri, A.P., 2017. Warm pool/cold tongue El Niño and Indian winter Monsoon. Meteorology and Atmospheric Physics, 129(3): 321-331.

Fan, F., Dong, X., Fang, X., Xue, F., Zheng, F. and Zhu, J., 2017. Revisiting the relationship between the South Asian summer monsoon drought and El Niño warming pattern. Atmospheric Science Letters, 18(4): 175-182.

Feba, F., Ashok, K. and Ravichandran, M., 2019. Role of changed Indo-Pacific atmospheric circulation in the recent disconnect between the Indian summer monsoon and ENSO. Climate Dynamics, 52(3-4): 1461-1470.

Freund, M.B., Henley, B.J., Karoly, D.J., McGregor, H.V., Abram, N.J. and Dommenget, D., 2019. Higher frequency of Central Pacific El Niño events in recent decades relative to past centuries. Nature Geoscience, 12(6): 450-455.

Gadgil, S., Vinayachandran, P.N., Francis, P.A. and Gadgil, S., 2004. Extremes of the Indian summer monsoon rainfall, ENSO and equatorial Indian Ocean oscillation. Geophysical Research Letters, 31(12).

Gautam, R., Hsu, N.C., Lau, K.M. and Kafatos, M., 2009, September. Aerosol and rainfall variability over the Indian monsoon region: distributions, trends and coupling. In Annales Geophysicae Copernicus GmbH, 27(9): 3691-3703.

Geethalakshmi, V., Yatagai, A., Palanisamy, K. and Umetsu, C., 2009. Impact of ENSO and the Indian Ocean Dipole on the north-east monsoon rainfall of Tamil Nadu State in India. Hydrological Processes: An International Journal, 23(4): 633-647.

Goswami, B.N., 1998. Interannual variations of Indian summer monsoon in a GCM: External conditions versus internal feedbacks. Journal of Climate, 11(4): 501-522.

Goswami, B.N., Madhusoodanan, M.S., Neema, C.P. and Sengupta, D., 2006. A physical mechanism for North Atlantic SST influence on the Indian summer monsoon. Geophysical Research Letters, 33(2).

Guhathakurta, P., Sreejith, O.P. and Menon, P.A., 2011. Impact of climate change on extreme rainfall events and flood risk in India. Journal of earth system science, 120(3), p.359.

Guo, Y.P. and Li, J.P., 2016. Impact of ENSO events on the interannual variability of Hadley circulation extents in boreal winter. Advances in Climate Change Research, 7(1-2): 46-53.

Halpern, D. and Woiceshyn, P.M., 2001. Somali jet in the Arabian Sea, El Niño, and India rainfall. Journal of Climate, 14(3): 434-441.

Ham, Y.G., Choi, J.Y. and Kug, J.S., 2017. The weakening of the ENSO–Indian Ocean Dipole (IOD) coupling strength in recent decades. Climate Dynamics, 49(1-2): 249-261.

Handler, P., 1986. Stratospheric aerosols and the Indian monsoon. Journal of Geophysical Research: Atmospheres, 91(D13): 14475-14490.

Hu, Y., Huang, H. and Zhou, C., 2018. Widening and weakening of the Hadley circulation under global warming. Science Bulletin, 63(10): 640-644.

Ihara, C., Kushnir, Y., Cane, M.A. and De la Pena, V.H., 2007. Indian summer monsoon rainfall and its link with ENSO and Indian Ocean climate indices. International Journal of Climatology: A Journal of the Royal Meteorological Society, 27(2): 179-187.

Kalnay, E., Kanamitsu, M., Kistler, R., Collins, W., Deaven, D., Gandin, L., Iredell, M., Saha, S., White, G., Woollen, J. and Zhu, Y., 1996. The NCEP/NCAR 40-year reanalysis project. Bulletin of the American meteorological Society, 77(3): 437-472.

Kao, H.Y. and Yu, J.Y., 2009. Contrasting eastern-Pacific and central-Pacific types of ENSO. Journal of Climate, 22(3): 615-632.

Kawamura, R., Uemura, K. and Suppiah, R., 2005. On the recent change of the Indian summer monsoon-ENSO relationship. SOLA, 1, pp.201-204.

Kinter III, J.L., Miyakoda, K. and Yang, S., 2002. Recent change in the connection from the Asian monsoon to ENSO. Journal of Climate, 15(10), pp.1203-1215.

Kishore, P., Jyothi, S., Basha, G., Rao, S.V.B., Rajeevan, M., Velicogna, I. and Sutterley, T.C., 2016. Precipitation climatology over India: validation with observations and reanalysis datasets and spatial trends. Climate dynamics, 46(1-2): 541-556.

Konwar, M., Parekh, A. and Goswami, B.N., 2012. Dynamics of east-west asymmetry of Indian summer monsoon rainfall trends in recent decades. Geophysical research letters, 39(10).

Krishnan, R. and Sugi, M., 2003. Pacific decadal oscillation and variability of the Indian summer monsoon rainfall. Climate Dynamics, 21(3-4): 233-242.

Krishnaswamy, J., Vaidyanathan, S., Rajagopalan, B., Bonell, M., Sankaran, M., Bhalla, R.S. and Badiger, S., 2015. Non-stationary and non-linear influence of ENSO and Indian Ocean Dipole on the variability of Indian monsoon rainfall and extreme rain events. Climate Dynamics, 45(1-2): 175-184.

Kug, J.S., Jin, F.F. and An, S.I., 2009. Two types of El Niño events: cold tongue El Niño and warm pool El Niño. Journal of Climate, 22(6): 1499-1515

Kumar, K.K., Rajagopalan, B. and Cane, M.A., 1999. On the weakening relationship between the Indian monsoon and ENSO. Science, 284(5423): 2156-2159.

Kumar, K.K., Rajagopalan, B., Hoerling, M., Bates, G. and Cane, M., 2006. Unraveling the mystery of Indian monsoon failure during El Niño. Science, 314(5796): 115-119.

L'Heureux, M.L., Takahashi, K., Watkins, A.B., Barnston, A.G., Becker, E.J., Di Liberto, T.E., Gamble, F., Gottschalck, J., Halpert, M.S., Huang, B. and Mosquera-Vásquez, K., 2017. Observing and predicting the 2015/16 El Niño. Bulletin of the American Meteorological Society, 98(7): 1363-1382.

Lee, T. and McPhaden, M.J., 2010. Increasing intensity of El Niño in the central-equatorial Pacific. Geophysical Research Letters, 37(14).

Lengaigne, M., Guilyardi, E., Boulanger, J.P., Menkes, C., Delecluse, P., Inness, P., Cole, J. and Slingo, J., 2004. Triggering of El Niño by westerly wind events in a coupled general circulation model. Climate Dynamics, 23(6): 601-620.

Liu, L., Yang, G., Zhao, X., Feng, L., Han, G., Wu, Y. and Yu, W., 2017. Why was the Indian Ocean dipole weak in the context of the extreme El Niño in 2015?. Journal of Climate, 30(12): 4755-4761.

Luo, J.J., Zhang, R., Behera, S.K., Masumoto, Y., Jin, F.F., Lukas, R. and Yamagata, T., 2010. Interaction between El Niño and extreme Indian ocean dipole. Journal of Climate, 23(3): 726-742.

Marjani, S., Alizadeh-Choobari, O. and Irannejad, P., 2019. Frequency of extreme El Niño and La Niña events under global warming. Climate Dynamics, 53(9-10): 5799-5813.

McPhaden, M.J., 2004. Evolution of the 2002/03 El Niño. Bulletin of the American Meteorological Society, 85(5): 677-696.

McPhaden, M.J., 2015. Playing hide and seek with El Niño. Nature Climate Change, 5(9): 791-795.

Meehl, G.A., 1987. The annual cycle and interannual variability in the tropical Pacific and Indian Ocean regions. Monthly Weather Review, 115(1): 27-50.

Meehl, G.A., Arblaster, J.M. and Collins, W.D., 2008. Effects of black carbon aerosols on the Indian monsoon. Journal of Climate, 21(12): 2869-2882.

Mishra, A.K., Dwivedi, S. and Das, S., 2020. Role of Arabian Sea warming on the Indian summer monsoon rainfall in a regional climate model. International Journal of Climatology, 40(4): 2226-2238.

Mishra, V., Smoliak, B.V., Lettenmaier, D.P. and Wallace, J.M., 2012. A prominent pattern of year-to-year variability in Indian Summer Monsoon Rainfall. Proceedings of the National Academy of Sciences, 109(19): 7213-7217.

Nair, P.J., Chakraborty, A., Varikoden, H., Francis, P.A. and Kuttippurath, J., 2018. The local and global climate forcings induced inhomogeneity of Indian rainfall. Scientific reports, 8(1): 1-12.

Nicholson, S.E. and Selato, J.C., 2000. The influence of La Niña on African rainfall. International Journal of Climatology: A Journal of the Royal Meteorological Society, 20(14): 1761-1776.

Nikumbh, A.C., Chakraborty, A. and Bhat, G.S., 2019. Recent spatial aggregation tendency of rainfall extremes over India. Scientific reports, 9(1): 1-7.

Ñiquen, M. and Bouchon, M., 2004. Impact of El Niño events on pelagic fisheries in Peruvian waters. Deep sea research part II: topical studies in oceanography, 51(6-9): 563-574.

Paek, H., Yu, J.Y. and Qian, C., 2017. Why were the 2015/2016 and 1997/1998 extreme El Niños different?. Geophysical Research Letters, 44(4): 1848-1856.

Pai, D.S., Sridhar, L., Badwaik, M.R. and Rajeevan, M., 2015. Analysis of the daily rainfall events over India using a new long period (1901–2010) high resolution (0.25× 0.25) gridded rainfall data set. Climate dynamics, 45(3-4): 755-776.

Pant, G.B. and Parthasarathy, S.B., 1981. Some aspects of an association between the southern oscillation and Indian summer monsoon. Archives for meteorology, geophysics, and bioclimatology, Series B, 29(3): 245-252.

Pattanaik, D.R. and Rajeevan, M., 2010. Variability of extreme rainfall events over India during southwest monsoon season. Meteorological Applications: A journal of forecasting, practical applications, training techniques and modelling, 17(1): 88-104.

Philander, S.G., 1998. Who is El Niño?. Eos, Transactions American Geophysical Union, 79(13): 170-170.

Philander, S.G.H., 1985. El Niño and La Niña. Journal of the Atmospheric Sciences, 42(23): 2652-2662.

Pillai, P.A. and Chowdary, J.S., 2016. Indian summer monsoon intra-seasonal oscillation associated with the developing and decaying phase of El Niño. International Journal of Climatology, 36(4): 1846-1862.

Rajeevan, M. and Pai, D.S., 2007. On the El Niño-Indian monsoon predictive relationships. Geophysical Research Letters, 34(4).

Rajeevan, M., Bhate, J. and Jaswal, A.K., 2008. Analysis of variability and trends of extreme rainfall events over India using 104 years of gridded daily rainfall data. Geophysical research letters, 35(18).

Rajeevan, M., Gadgil, S. and Bhate, J., 2010. Active and break spells of the Indian summer monsoon. Journal of earth system science, 119(3): 229-247.

Rao, S.A., Chaudhari, H.S., Pokhrel, S. and Goswami, B.N., 2010. Unusual central Indian drought of summer monsoon 2008: role of southern tropical Indian Ocean warming. Journal of climate, 23(19): 5163-5174.

Ratnam, J.V., Behera, S.K., Masumoto, Y., Takahashi, K. and Yamagata, T., 2010. Pacific Ocean origin for the 2009 Indian summer monsoon failure. Geophysical research letters, 37(7).

Rayner, N.A.A., Parker, D.E., Horton, E.B., Folland, C.K., Alexander, L.V., Rowell, D.P., Kent, E.C. and Kaplan, A., 2003. Global analyses of sea surface temperature, sea ice, and night marine air temperature since the late nineteenth century. Journal of Geophysical Research: Atmospheres, 108(D14).

Revadekar, J.V. and Kulkarni, A., 2008. The El Niño-Southern Oscillation and winter precipitation extremes over India. International Journal of Climatology: A Journal of the Royal Meteorological Society, 28(11): 1445-1452.

Revadekar, J.V., Kothawale, D.R. and Rupa Kumar, K., 2009. Role of El Niño/La Niña in temperature extremes over India. International Journal of Climatology: A Journal of the Royal Meteorological Society, 29(14): 2121-2129.

Rohini, P., Rajeevan, M. and Srivastava, A.K., 2016. On the variability and increasing trends of heat waves over India. Scientific reports, 6(1): 1-9.

Roxy, M.K. and Chaithra, S.T., 2018. Impacts of Climate Change on the Indian Summer Monsoon. Ministry of Environment, Forest and Climate Change (MoEF&CC), Government of India.

Roxy, M.K., Ghosh, S., Pathak, A., Athulya, R., Mujumdar, M., Murtugudde, R., Terray, P. and Rajeevan, M., 2017. A threefold rise in widespread extreme rain events over central India. Nature communications, 8(1): 1-11.

Roxy, M.K., Ritika, K., Terray, P. and Masson, S., 2014. The curious case of Indian Ocean warming. Journal of Climate, 27(22): 8501-8509.

Roxy, M.K., Ritika, K., Terray, P., Murtugudde, R., Ashok, K. and Goswami, B.N., 2015. Drying of Indian subcontinent by rapid Indian Ocean warming and a weakening land-sea thermal gradient. Nature communications, 6(1): 1-10.

Sabeerali, C.T., Ajayamohan, R.S., Bangalath, H.K. and Chen, N., 2019. Atlantic Zonal Mode: An Emerging Source of Indian Summer Monsoon Variability in a Warming World. Geophysical Research Letters, 46(8): 4460-4467.

Saji, N.H., Goswami, B.N., Vinayachandran, P.N. and Yamagata, T., 1999. A dipole mode in the tropical Indian Ocean. Nature, 401(6751): 360-363.

Sanap, S.D., Priya, P., Sawaisarje, G.K. and Hosalikar, K.S., 2019. Heavy rainfall events over southeast peninsular India during northeast monsoon: Role of El Niño and easterly wave activity. International Journal of Climatology, 39(4): 1954-1968.

Sarkar, S., Singh, R.P. and Kafatos, M., 2004. Further evidences for the weakening relationship of Indian rainfall and ENSO over India. Geophysical research letters, 31(13).

Shukla, R.P. and Huang, B., 2016. Interannual variability of the Indian summer monsoon associated with the air–sea feedback in the northern Indian Ocean. Climate dynamics, 46(5-6): 1977-1990.

Singh, P., Gnanaseelan, C. and Chowdary, J.S., 2017. North-East monsoon rainfall extremes over the southern peninsular India and their association with El Niño. Dynamics of Atmospheres and Oceans, 80: 1-11.

Slingo, J.M. and Annamalai, H., 2000. 1997: The El Niño of the century and the response of the Indian summer monsoon. Monthly Weather Review, 128(6): 1778-1797.

Sreenivas, P., Gnanaseelan, C. and Prasad, K.V.S.R., 2012. Influence of El Niño and Indian Ocean Dipole on sea level variability in the Bay of Bengal. Global and Planetary Change, 80: 215-225.

Suthinkumar, P.S., Babu, C.A. and Varikoden, H., 2019. Spatial Distribution of Extreme Rainfall Events During 2017 Southwest Monsoon over Indian Subcontinent. Pure and Applied Geophysics, 176(12): 5431-5443.

Taraphdar, S., Mukhopadhyay, P. and Goswami, B.N., 2010. Predictability of Indian summer monsoon weather during active and break phases using a high resolution regional model. Geophysical research letters, 37(21).

Tomillo, P.S., Fonseca, L.G., Ward, M., Tankersley, N., Robinson, N.J., Orrego, C.M., Paladino, F.V. and Saba, V.S., 2020. The impacts of extreme El Niño events on sea turtle nesting populations. Climatic Change, 159(2): 163-176.

Torrence, C. and Compo, G.P., 1998. A practical guide to wavelet analysis. Bulletin of the American Meteorological society, 79(1): 61-78.

Ummenhofer, C.C., Gupta, A.S., Li, Y., Taschetto, A.S. and England, M.H., 2011. Multi-decadal modulation of the El Niño–Indian monsoon relationship by Indian Ocean variability. Environmental Research Letters, 6(3), p.034006.

Varikoden, H. and Preethi, B., 2013. Wet and dry years of Indian summer monsoon and its relation with Indo-Pacific sea surface temperatures. International journal of climatology, 33(7): 1761-1771.

Varikoden, H. and Revadekar, J.V., 2020. On the extreme rainfall events during the southwest monsoon season in northeast regions of the Indian subcontinent. Meteorological Applications, 27(1), p.e1822.

Varikoden, H., Kumar, K.K. and Babu, C.A., 2013. Long term trends of seasonal and monthly rainfall in different intensity ranges over Indian subcontinent. Mausam, 64(3): 481-488.

Varikoden, H., Revadekar, J.V., Choudhary, Y. and Preethi, B., 2015. Droughts of Indian summer monsoon associated with El Niño and Non-El Niño years. International Journal of Climatology, 35(8): 1916-1925.

Varikoden, H., Revadekar, J.V., Kuttippurath, J. and Babu, C.A., 2019. Contrasting trends in southwest monsoon rainfall over the Western Ghats region of India. Climate Dynamics, 52(7-8): 4557-4566.

Vellore, R.K., Krishnan, R., Pendharkar, J., Choudhury, A.D. and Sabin, T.P., 2014. On the anomalous precipitation enhancement over the Himalayan foothills during monsoon breaks. Climate dynamics, 43(7-8): 2009-2031.

Vernekar, A.D., Zhou, J. and Shukla, J., 1995. The effect of Eurasian snow cover on the Indian monsoon. Journal of Climate, 8(2): 248-266.

Vishnu, S., Francis, P.A., Shenoi, S.C. and Ramakrishna, S.S.V.S., 2018. On the relationship between the Pacific Decadal Oscillation and monsoon depressions over the Bay of Bengal. Atmospheric Science Letters, 19(7), p.e825.

Vishnu, S., Francis, P.A., Shenoi, S.S.C. and Ramakrishna, S.S.V.S., 2016. On the decreasing trend of the number of monsoon depressions in the Bay of Bengal. Environmental Research Letters, 11(1), p.014011.

Webster, P.J., Moore, A.M., Loschnigg, J.P. and Leben, R.R., 1999. Coupled ocean–atmosphere dynamics in the Indian Ocean during 1997–98. Nature, 401(6751): 356-360.

Weng, H., Ashok, K., Behera, S.K., Rao, S.A. and Yamagata, T., 2007. Impacts of recent El Niño Modoki on dry/wet conditions in the Pacific rim during boreal summer. Climate dynamics, 29(2-3): 113-129.

Wu, R. and Kirtman, B.P., 2003. On the impacts of the Indian summer monsoon on ENSO in a coupled GCM. Quarterly Journal of the Royal Meteorological Society: A journal of the atmospheric sciences, applied meteorology and physical oceanography, 129(595): 3439-3468.

Xavier, P.K., Marzin, C. and Goswami, B.N., 2007. An objective definition of the Indian summer monsoon season and a new perspective on the ENSO–monsoon relationship. Quarterly Journal of the Royal Meteorological Society: A journal of the atmospheric sciences, applied meteorology and physical oceanography, 133(624): 749-764.

Yadav, R.K., Ramu, D.A. and Dimri, A.P., 2013. On the relationship between ENSO patterns and winter precipitation over North and Central India. Global and planetary change, 107: 50-58.

Yamagata, T., Behera, S.K., Luo, J.J., Masson, S., Jury, M.R. and Rao, S.A., 2004. Coupled ocean-atmosphere variability in the tropical Indian

Ocean. Earth's Climate: The Ocean–Atmosphere Interaction, Geophys. Monogr, 147: 189-212.

Zheng, Y., Bourassa, M.A. and Ali, M.M., 2020. Statistical evidence on distinct impacts of short-and long-time fluctuations of Indian Ocean surface wind fields on Indian summer monsoon rainfall during 1991–2014. Climate Dynamics, 54(5): 3053-3076.

Zubair, L. and Ropelewski, C.F., 2006. The strengthening relationship between ENSO and northeast monsoon rainfall over Sri Lanka and southern India. Journal of Climate, 19(8): 1567-1

EXTREME ENSO (El Nino Southern Oscillation) EVENTS

AND

MONSOON VARIABILITY OVER INDIA

by

ATHIRA K.S

(2015-20-023)

ABSTRACT OF THE THESIS

submitted in partial fulfilment of the

requirement of the degree of

B. Sc.-M. Sc. (Integrated) Climate Change Adaptation

Faculty of Agriculture

Kerala Agricultural University

ACADEMY OF CLIMATE CHANGE EDUCATION AND RESEARCH

VELLANIKKARA, THRISSUR - 680 656

KERALA, INDIA,

2020

ABSTRACT

El Niño Southern Oscillation refers to the coupled ocean atmospheric phenomena that is generated in the tropical Pacific Ocean on an approximate timescale of 2-7 years. The periodic warming and cooling are called El Niño and La Niña respectively. El Niño events are characterized by warmer than normal SST over the central and eastern Pacific Ocean whereas La Niña events are marked by cooler than normal SST. There is a drastic reduction in the amount of Indian summer monsoon rainfall in response to El Niño. The opposite is true for La Niña conditions. It was found out that the connection between ENSO and the monsoon is not uniform for the entire Indian subcontinent for the period of study from 1901 to 2018. It started rising from 1901, then became stable for the period 1940 to 1980 and decreased for the recent period. Based on the variability in the relationship, three regions- namely north, central and south India were selected which exhibit moderate, high and consistent relationship with ENSO respectively. ENSO and monsoon trough/depressions were identified to be the major drivers of ISMR variability. The effect of these were checked for north, central and south India rainfall. North India has an increasing dependency on ENSO while the influence of monsoon trough/depression is declining. Central India is dependent mainly on monsoon trough/depressions. South India has its relation on ENSO as well as monsoon trough/depressions. Hence it is due to the rising influence of monsoon trough/depression that the ENSO-monsoon interrelationship has decreased in central India.

The study of the impacts of extreme ENSO events on ISMR revealed that very strong El Niño years influenced only north and south India. The central India rainfall was particularly high during this time such that extreme rainfall events were also identified. The result was opposite at the time of very strong La Niña events which brought heavy rainfall to north and south India but low rainfall in Central India.